ISSN 0252-1075
Research Report No. RR-091

Contribution from
Indian Institute of Tropical Meteorology

MODELLING STUDIES OF THE 2000 INDIAN SUMMER MONSOON AND EXTENDED ANALYSIS

by

KRISHNAN R., MUJUMDAR M.,
VAIDYA V., RAMESH K.V.
and
SATYAN V.

PUNE – 411 008
INDIA

DECEMBER 2001

Contents

Modelling Studies of the 2000 Indian Summer Monsoon and Extended Analysis

R.Krishnan, M.Mujumdar, V.Vaidya, K.V.Ramesh and V.Satyan

Indian Institute of Tropical Meteorology, Pune 411 008, India.

ABSTRACT

Diagnostic analysis of observations and a series of ensemble simulations using an atmospheric general circulation model (GCM) have been carried out with a view to examine the widespread suppression of the seasonal summer monsoon rainfall over the Indian subcontinent in 2000. During this period, the equatorial and southern tropical Indian Ocean was characterized by warmer than normal sea surface temperature (SST), increased atmospheric moisture convergence and enhanced precipitation. These abnormal conditions not only offered an ideal prototype of the regional convective anomalies over the subcontinent and Indian Ocean; but also provided a basis for investigating into the causes for intensification and maintenance of the anomaly patterns. The findings of this study reveal that the strengthening of the convective activity over the region of the southern equatorial trough played a key role in inducing anomalous subsidence over the subcontinent and thereby weakened the monsoon Hadley cell. It is shown that the leading Empirical Orthogonal Function (EOF) component of the intraseasonal variability of observed rainfall was characterized by a north-south asymmetric pattern of negative anomaly over India and positive anomaly over the equatorial belt. This first EOF accounted for about 21 % of the total rainfall variance during 2000. GCM simulations suggest that the break monsoon pattern of rainfall anomaly tends to intensify and persist in presence of warm tropical Indian Ocean SST anomalies as in 2000. By further extending the analysis of observed records over a 22-year (1979-2000) period, we have objectively delineated several deficient monsoon rainfall seasons (eg., 1979, 1986, 1987, 1995, 2000) during which the out-of-phase pattern of intraseasonal variability over the subcontinent and the equatorial Indian Ocean seems to have been reinforced in response to warm SST anomalies in the tropical Indian Ocean. These results underline the premise for indepth exploration of the physical link between the tropical Indian Ocean SST, the near-equatorial convective activity and the large-scale atmospheric dynamics; and offer scope for understanding some of the intriguing peculiarities of convection over the monsoon region.

1 Introduction

The South Asian summer monsoon circulation, occurring every year from June to September, is one of the most spectacular seasonal phenomenon on this globe. Despite the remarkable consistency in the seasonal reversal of the wind patterns, it is well-known that the summer monsoon rainfall over the Indian subcontinent exhibits considerable interannual variability (Parthasarathy, *et al.*, 1995). Particularly noteworthy is the recent case of abnormally low Indian monsoon rainfall in 2000. Severe drought conditions prevailed over a large area covering the plains of Central and North India where the monsoon rainfall was deficient by more than 25 % of the normal (Fig.1a). The total rainfall for the monsoon season of 2000 over the whole of the country was about 8 % below the long-term climatological normal[1]. There are several compelling reasons for undertaking the 2000 monsoon case-study. Firstly, the precipitation decrease was wide-spread in spatial extent. Extreme drought conditions were not confined merely to the plains of north-central India but also extended over areas of Pakistan (http://met.gov.pk/drought) so that the large rainfall reduction by the end of September 2000 produced an adverse impact on the water availability over the South Asian region (http://www.fao.org/). The second important aspect was the occurrence of prolonged break (inactive) rainfall spells during the 2000 monsoon season. The daily time-series of the All India summer monsoon precipitation (Fig.1b) shows three major break spells (*i.e.*, the first one in the third week of June; the second was an intense and long dry spell extending from third week of July until the second week of August; and the next break spell lasted during the second and third weeks of September). The seasonal mean monsoon rainfall during a given year is known to be crucially determined by the active/break rainfall spells associated with the intraseasonal fluctuations of the monsoon (Goswami and Ajaya Mohan, 2001). Therefore, it is pertinent to examine the agents that were responsible for inducing the long-lasting behavior of the monsoon break spells in 2000.

The third point about the 2000 summer monsoon is the nature of tropical SSTs that prevailed during that season. It is known that a majority of monsoon droughts in the past have occurred in conjunction with El Niño events in the Pacific Ocean (Sikka, 1999). Previous studies have pointed out that enhanced convection associated with warm SST anomalies in the tropical central-eastern Pacific Ocean can induce anomalous subsidence of the east-west Walker circulation over the Indian region and thereby suppress the monsoon rainfall (Palmer *et al.*, 1992). Numerous studies have documented the relationship between El Niño/ Southern Oscillation (ENSO) and the Indian monsoon rainfall (Pant and Parthasarathy, 1981; Rasmusson and Carpenter, 1983, Shukla and Paolino, 1983). In contrast to most of the earlier droughts, the wide-spread decrease of monsoon rainfall in 2000 was however, not related to El Niño conditions in the Pacific ocean. The absence of an El Niño event during 2000 is clearly evident from the plot of observed SST anomalies (Fig.2) which shows weak negative anomalies in the equatorial central-eastern Pacific Ocean. On the other hand, the tropical Indian Ocean was characterized by warm SST anomalies extending longitudinally across much of the ocean basin. The maximum value of the SST anomaly around 55-65 °E to the south of the equator was close to 1°C. Warm SST anomalies can also be noticed to the south of 10°S in the central-eastern Indian Ocean in Fig.2. By examining the monthly fields, we have

[1]The India Meteorological Department defines a monsoon drought when the All India Summer Monsoon rainfall during a given year is deficient by more than 10 % of the climatological normal.

confirmed that the positive SST anomalies in the tropical Indian Ocean persisted during the entire monsoon season.

Convection variability over the tropical Indian Ocean and the monsoon region remain ambiguous in many aspects. For instance, while it is known that convection tends to increase over the equatorial Indian Ocean during monsoon breaks (Krishnan *et al.*, 2000), it is not clear as to how the distribution of convection patterns during monsoon breaks is affected by SST anomalies in the Indian Ocean. One of the main reasons behind the complexity of this problem arises on account of the inherent nonlinear relationships among SST, convection and atmospheric dynamics (Zhang, 1993). Nevertheless, the situation that prevailed during 2000 provided an excellent opportunity to examine some of the regional issues in greater depth. Especially, the occurrence of prolonged monsoon breaks over India, in combination with the warm SST anomalies in the tropical Indian Ocean and the lack of El Niño conditions in the Pacific Ocean, offered a naturally conducive setting to concentrate on the impact of the Indian Ocean SST anomalies on the regional scale convection. In the past, there have been a few studies dealing with the influence of Indian Ocean SST anomalies on the summer monsoon. Shukla (1975) examined the impact of cold SST anomalies, in the western Arabian Sea and the Somali coast, on the monsoon circulation and rainfall. His results showed a decrease of rainfall over India which he attributed to a decrease of local evaporation and reduction in the cross equatorial moisture flux. Washington *et al.*, (1977) studied the summer monsoon response to different types of idealized SST anomalies in the tropical Indian Ocean. Their results indicated an increase in rainfall and vertical velocity over the warm SST anomaly. However the simulated monsoon rainfall and wind anomalies obtained in their experiments were not statistically significant. Recently, Chandrasekar and Kitoh (1998) carried out experiments using the Meteorological Research Institute (MRI) GCM in order to study the sensitivity of the monsoon circulation and rainfall to anomalous SST in tropical Indian Ocean. They noted that rainfall increased (decreased) over the Indian Ocean region of warm (cold) SST anomaly. In contrast, the seasonal rainfall over the Indian land region showed a decrease (increase); accompanied by a weakening (strengthening) of the cross-equatorial flow in their warm (cold) SST anomaly experiment. One of the shortcomings of their study was the lack of observational justification for the idealized Indian Ocean SST anomaly which was held fixed in their model integrations. Since a GCM response can be quite sensitive to the distribution of SST, it is essential that the specified SST boundary forcing is as realistic as possible so that the model simulation can be evaluated objectively (Palmer *et al.*, 1992). Secondly, Chandrasekar and Kitoh (1998) only speculated about the possible impact of SST anomalies on the convection over the monsoon region; however their model simulations did not explicitly provide an explanation for the modifications of the intraseasonal active/break monsoon spells on account of the SST forcing. From the above discussions, one can realize the need to provide a consistent description of the intraseasonal variability of the monsoon rainfall and its link with SST and convection anomalies over the tropical Indian Ocean.

The primary objective of this paper is to understand the factors that contributed to the maintenance of the anomalous features associated with the monsoon drought-like situation over India in 2000. One of the key issues in this context, is concerning the influence of the warm tropical Indian Ocean SST anomalies both on the large-scale monsoon circulation as well as on the regional-scale intraseasonal convection. In particular, special attention has

been paid towards assessing the sensitivity of monsoon breaks to the Indian Ocean SST forcing. Keeping these goals in mind, we have adopted a two-fold strategy that combines both diagnostic analysis of observed datasets and also numerical experiments using an atmospheric GCM. Besides the 2000 monsoon case-study, we have additionally extended our analysis of the observed records over a 22-year (1979-2000) period in order to obtain a general perspective about the possible ramifications of the Indian Ocean SST forcing on the atmospheric convection overlying the ocean surface and that over the monsoon region.

a. Datasets used

Datasets from multiple sources have been employed for the present analysis. They consist of the sub-divisional and All India rainfall prepared by Indian Institute of Tropical Meteorology (IITM); the gridded rainfall dataset both over land and oceanic areas from the Climate Prediction Center (CPC) - which is commonly referred to as the CPC Merged Analysis of Precipitation (CMAP). The CMAP dataset is a product of merging raingauge observations and precipitation estimates from satellites (Xie and Arkin, 1997). The SST data used for our analysis is based on the Optimum Interpolated SST (OISST) which uses insitu and satellite derived SSTs plus SSTs simulated by sea-ice cover (Reynolds and Smith, 1994). Atmospheric parameters such as (winds, moisture, vertical velocity, etc) were obtained from the National Center for Environmental Prediction (NCEP) reanalysis dataset (Kalnay *et al.,* 1996). We have also used in our analysis, the daily time-series of All India rainfall; along with the daily interpolated data of Outgoing Longwave Radiation (OLR) for a 22-year (1979-2000) period. The daily All India rainfall data, based on rainfall from stations over India, for all these years was obtained from the India Meteorological Department (IMD); the OLR data from National Oceanic Atmospheric Administration (NOAA) satellite was provided by the Climate Diagnostic Center, Boulder, Colorado. Maps of sea-level departures during 2000 monsoon season based on insitu observations over Indian stations obtained from IMD are also presented. In addition, we have gathered reports of rainfall departures from Monthly Climate Data for the World.

b. Model details

The summer monsoon response to the Indian Ocean SST anomalies during 2000 has been examined by carrying out four sets of 10-member ensemble integrations using the Center for Ocean-Land-Atmosphere (COLA) GCM. The four sets of experiments differ from each other with regard to the specification of the SST boundary forcing (see Table.1). The rationale behind carrying out the four sets of experiments is described in section3. Each of these four sets, in turn comprises of ten realizations in which the GCM was integrated starting from ten different initial conditions. The details of these initial and boundary conditions are presented in Table.1. The observed global atmospheric conditions from NCEP reanalysis for 10 continuous days (22-31 May, 2000) are processed in order to obtain the multiple initial conditions necessary for performing the ensemble runs. The SST used for prescribing the boundary condition in the GCM is based on the observed OISST (Reynolds and Smith, 1994). The COLA GCM is a spectral model with horizontal resolution truncated at wavenumber 30 (T30) and consists of 18 unevenly spaced sigma levels in the vertical. The complete documentation of the model framework and the physical parameterization schemes used in the GCM are provided by Kinter *et al.,* (1997). This GCM has been extensively used for monsoon studies (e.g. Fennessy *et al.,* 1994; Krishnan *et al.*, 1998, Kirtman and Shukla, 2000, Mujumdar and Krishnan, 2001).

2 Data analyses

2.1 Seasonal features

The South Asian monsoon circulation is classically portrayed as a gigantic sea breeze *ie.*, a meridional Hadley cell (Krishnamurti, 1986) driven by atmospheric differential heating between the Asian land mass (to the north) and the oceans (to the south). The Tibetan plateau acts as an elevated heat source and produces an explosive warming of the troposphere during the northern summer (Yanai, *et al.,* 1992). Water vapor is transported into the subcontinent by the Somali jet and the cross-equatorial flow from the Indian Ocean (Saha and Bavadekar, 1973; Rao and Van de Boogard, 1981 and Cadet and Reverdin, 1981). Moisture is carried upward by the monsoon convection, so that it condenses and warms the upper troposphere where a strong anticyclone develops. Various rain producing systems like the onset vortex, monsoon depressions, mid-tropospheric cyclones bring copious rainfall over the Indian region during the June to September months (Krishnamurti, 1985). The spatial distribution of the observed seasonal mean precipitation (Fig.3a) shows two rainfall maxima - one over the Bay of Bengal and the other over the west coast of India. A secondary rainfall maximum is located over the equatorial Indian Ocean. Also illustrated in Fig.3a is the transport of water vapor from the oceanic areas into the Indian region by the cross-equatorial winds and southwest monsoon flow. The monsoon Hadley circulation is depicted by the meridional -vertical section of atmospheric circulation in Fig.3b. The ascending branch of the Hadley cell is located around 25°N and the descending branch of the Hadley cell can be seen in the southern Indian Ocean. This circulation is associated with southerlies in the lower levels and northerlies in the upper troposphere.

The anomalies of precipitation and moisture transport vector for the monsoon 2000 season are shown in Fig.3c. Large negative rainfall anomalies can be seen over the eastern Arabian Sea, west coast of India, central and southern Bay of Bengal. Also prominently seen is the rainfall decrease over north-central India by as much as 2-3 mm day^{-1}. The small pocket of increased rainfall over the northeast region is a typical feature known to be associated with weakening of the monsoon activity (Ramamurthy, 1969, Dhar *et al.,* 1984, Krishnamurthy and Shukla, 2001). The wide-spread reduction of rainfall over the plains of India shown by the CMAP dataset (Fig.3c) is broadly consistent with the precipitation anomalies in Fig.1a which are entirely based on observed insitu rainfall over Indian stations. The moisture transport vector (Fig.3c) reveals anomalous easterlies over the Arabian Sea, the Indian subcontinent, the Bay of Bengal, Burma, Thailand and Vietnam indicative of the decrease of water vapor influx into the monsoon region. This restricted moisture transport and the anticyclonic anomaly over western India and the Arabian Sea corroborate with the rainfall suppression over the region. A conspicuous feature in Fig.3c is the elongated band of increased rainfall over the tropical Indian Ocean during the summer of 2000. This anomalous patch with magnitude as large as 1.5 mmday^{-1} is located between the equator and 10°S and extends eastward from about 60°E as far as the Indonesian islands and the west Pacific. The (y-p) section (Fig.3d) illustrates anomalous upward motions to the south (10-20°S) of the equator and compensating

subsidence over the northern side (10-20°N). The above changes in the Hadley cell provide dynamical support to the opposite polarity of convective anomalies over the Indian landmass and the equatorial ocean.

The contrasting nature of the north-south asymmetric anomalies can be confirmed by additional analysis of the moisture transport vector. Earlier studies have shown the importance of decomposing the water vapor transport vector into non-divergent and divergent components (Chen 1985; Krishnan, 1998). The non-divergent (or rotational) part represents the transport term; while the divergent part describes the distribution of moisture convergence. We have computed these two terms using the classical Helmoltz theorm (Chen 1985; Krishnan 1998). The plots in Fig.4(a,b) show the anomalies of the rotational ($\vec{Q}_\psi$) and divergent ($\vec{Q}_\chi$) components during 2000. The $\vec{Q}_\psi$ component (Fig.4a) shows a prominent anticyclonic anomaly to the north of the equator. The large-scale reduction of moisture transport by the monsoon flow is clearly evident from the anomalous easterlies extending from the Arabian Sea, India, Bay of Bengal, Indochina and further eastward. The anomalous clockwise circulation located between 70-100°E in the Southern Hemisphere represents a cyclonic anomaly that is consistent with the increased oceanic convection. The ($\vec{Q}_\chi$) term (Fig.4b) shows anomalous divergent outflow of moisture over the Indian subcontinent and East Asia; but anomalous convergence of moisture over the Southern Indian Ocean. The anomalous potential function (χ_Q) consisting of negative (positive) anomalies to the north (south) of the equator distinctly shows the meridional antisymmetry of the divergent anomalies during 2000.

2.2 Monsoon intraseasonal variability

It is well-known that the southwest monsoon system exhibits vigorous intraseasonal fluctuations manifesting in the form of active/break rainfall spells (Krishnamurti and Bhalme, 1976; Yasunari, 1979; Sikka and Gadgil, 1980; Krishnamurti and Subrahmanyam, 1982; Krishnan *et al.*, 2000, Goswami and Ajaya Mohan, 2001). Here we examine the intraseasonal evolution of precipitation and low-level wind patterns over the Indian region during the 2000 summer monsoon season using the pentadal (5-day average) data of rainfall from CMAP, the (u, v) components of 850 hPa winds from NCEP reanalysis. It must be mentioned that the pentadal wind dataset was actually computed from the NCEP daily winds. The first step in our analysis was to construct a smoothly varying pentadwise climatology of rainfall and wind fields for all the 24 pentads that span the June-September months. For this purpose, we used the pentadal datasets of rainfall and 850 hpa winds available for 22 years (1979-2000). Climatologies were prepared for all of the 24 pentads by taking 22-year averages. We have verified that the pentadal climatology shows a realistic seasonal evolution of rainfall and low-level winds. In the next step, pentadal anomalies for the 2000 monsoon season were calculated by subtracting the climatology from the individual pentads of 2000.

We had earlier described the three major break spells that occurred during the 2000 monsoon season (Fig.1b). These three spells can be identified from the evolution of the anomaly patterns depicted in Fig.5. The first spell during the third week of June coincides with the anomaly patterns in pentads (34-35) which indicate negative rainfall anomalies and

low-level anticyclonic circulation anomaly over North-Central India and the Arabian Sea region. By back-tracking the evolution of the first break spell, one can note the development of a negative anomaly of rainfall (subdued convection) in pentad 31 over the southern Indian Ocean; this negative anomaly extends into the Bay of Bengal in pentads 32-33; and later moves northwestward quickly into central and north India in Pentad 34; and continues to persist in pentad 35. The northwest movement of suppressed convective anomalies, from the Bay of Bengal into the subcontinent, is a typical feature known to occur during monsoon breaks (Krishnan *et al.,* 2000). The second break was a prolonged spell lasting from the third week of July until about 10 August. Coincident with the timing of this long break we notice a prominent anticyclonic anomaly and a decrease in rainfall in pentads (41-44) over the plains of India, the Arabian Sea and the Bay of Bengal. A significant weakening of the southwest monsoon flow is evident from the easterly anomalies over the Indian region. The third spell in pentads (50-52) shows wide-spread rainfall reduction and strong anticyclonic anomalies over India. Apart from these three major breaks, there were periods of subdued monsoon activity in pentads (33,46,49). The agreement between the rainfall and wind patterns can also be noticed over the tropical Indian Ocean. For instance the cyclonic anomalies over the equatorial and southern Indian Ocean for pentads (35,43,52) are dynamically colocated with the enhanced rainfall anomalies in the region.

A quantitative assessment of the out-of-phase behavior of the intraseasonal convective anomalies over the subcontinent and the equatorial Indian Ocean during 2000 can be obtained by performing a Principal Component (PC) analysis of the CMAP pentadal rainfall anomalies. The PC/EOF technique involves expanding a space-time field in terms of linearly independent orthogonal basic functions. This analysis provides percentage contributions to the total variance explained by the different linearly independent components. The structure of the leading Empirical Orthogonal Function (EOF) in Fig.6a shows a pattern of negative anomalies over the Arabian Sea, Indian land region and the Bay of Bengal; and positive anomalies over the tropical Southern Indian Ocean. This first EOF pattern explains about 21% of the total variance. It is important to note that the independent contribution from the first EOF is not small in view of the fact that it accounts for variations over a large region which includes the subcontinent as well as the tropical Indian Ocean. We have examined the other EOF components as well. The structure of the second EOF showed decreased rainfall over India; however the increased rainfall over the equatorial Indian Ocean associated with the second EOF was not as prominent as in the case of the first EOF (figure not shown). The second EOF accounted for about 14 % of the total variance; while the contributions from the third and higher EOFs were less than 10 % individually. The time-series of the first PC (Fig.6b) indicates three peaks (A,B,C), which are found to match well the timing of the three major monsoon breaks. This result further substantiates that the monsoon breaks during 2000 were strongly linked to the fluctuations of intraseasonal convective activity over the tropical Indian Ocean. Based on a power spectrum analysis, we have verified that the first PC time-series shows spectral peaks around 15 days and 45 days. These two time-scales are reminiscent of the 10-20 day and 30-60 day oscillations of the monsoon system described by earlier studies (Krishnamurti and Bhalme, 1976; Dakshinamurthy and Keshavamurty, 1976; Yasunari, 1979, Krishnamurti and Subrahmanyam, 1982; Goswami and Ajaya Mohan, 2001).

2.3 Pressure departure charts during monsoon breaks

Daily observations of surface pressure over Indian stations are an important source of information for studying the development of monsoon breaks. During a break phase, the monsoon trough is known to shift northward from its normal position to the foothills of the Himalaya (Ramamurthy, 1969) resulting in above normal pressures, of the order of 4 hPa, over the plains of north-central India. The evolution of anomaly pressure patterns associated with the prolonged monsoon break that extended from the third week of July upto the second week of August 2000, is illustrated in the sequence of plots shown in Fig.7. The daily pressure departures for the period 18 July - 10 August 2000 were obtained from IMD. The pressure departures are essentially anomalies of surface pressure obtained by subtracting long-term climatological normals from insitu observations over Indian stations. In Fig.7a, one can note a negative pressure anomaly over the head Bay of Bengal and adjoining area on 18 July. This state is prior to the initiation of the monsoon break. In the next couple of days, the anomalous low moves north-westward and is located over northwest India on 21 July (Fig.7d). In the meanwhile, one notices the development of positive pressure anomalies over northeast India and Bay of Bengal on 21 July (Fig.7d). The high-pressure anomalies quickly move northwestward into central and north India on 22 July; the pressures are now higher than normal by 4 hPa (Fig.7e). This stage more or less marks the initiation of the monsoon break. The rapid northwest movement of the high-pressure anomaly pattern towards northwest India is consistent with the findings of Krishnan *et al.*, 2000 who pointed out that the triggering of monsoon breaks is preceded by rapid northwest movement of suppressed convection and high-pressure anomalies from the Bay of Bengal towards northwest India. It can be seen that the pressure anomalies further extend fully into northwest India on 23 July (Fig.7f). While there were some day-to-day variations, the high pressure anomalies in general continued to prevail over the country until around 8 August 2000. The break condition seems to weaken on 9 August 2000. At this stage one can notice the formation of low-pressure anomalies over the east coast and Bay of Bengal area. The above description of the pressure anomaly patterns provides additional confirmation for the longevity of the second major break spell which lasted nearly for 18 days (22 July - 08 August, 2000).

2.4 Enhancement of convection over the equatorial Indian Ocean

The picture emerging from the PC/EOF analysis (Fig.6) clearly demonstrated that the anomalous enhancement of convection over the warm tropical Indian ocean was a predominant feature during the 2000 monsoon season. The effect of SST on deep convection must be realized through modification of the dynamic and thermodynamic conditions in the atmospheric boundary layer and above. There have been studies suggesting that SSTs in excess of 27.5°C *are necessary but not sufficient* for the occurrence of deep convection over tropical oceans (Gadgil *et al.*, 1984; Graham and Barnett, 1987). The results of Zhang (1993) indicate that the variability of deep convection becomes larger for higher SST. He argued that factors unfavorable to convection can sometimes be so dominant as to suppress upward vertical motions inspite of high SST. According to Graham and Barnett (1987), the divergence of the surface winds is an important agent in determining the presence or absence of convection over high SST regions. In interpreting the connection between SST and convection over the Indian

Ocean, we draw attention to the study by Lindzen and Nigam (1987) who proposed that in areas of maximum SST, the surface moisture convergence induced by large-scale SST gradients in the tropics plays a crucial role in determining the distribution of convection and precipitation. They showed that SST as a boundary condition influences the moisture convergence at the surface, which together with fluxes of latent and sensible heat from the warm tropical oceans into the atmosphere, makes conditions more favorable for deep convection. Lindzen and Nigam (1987) particularly highlighted the importance of meridional gradients of SST in affecting the zonal winds over the tropical oceans. The latitudinal variation of the Indian Ocean SST anomalies during 2000 (Fig.8a) indicates that the equatorial and southern Indian Ocean (-10°S to 5°N) was warmer than the North Indian Ocean (5°N-15°N) by around 0.3-0.4°C or so. Earlier it was seen in (Fig.3c, Fig.4b) that the monsoon 2000 anomaly patterns exhibited increased convergence of moisture over the Southern tropical Indian Ocean; but anomalous divergence over the Indian land region. The latitudinal variation of the anomalous moisture divergence term (Fig.8b) indicates negative values to the south of 5°N implying enhanced convergence over this region; and positive values (anomalous divergence) to the north of 5°N. Thus the large-scale north-south variation of SST and moisture convergence anomalies during 2000 (Fig.8) are qualitatively consistent with the Lindzen-Nigam hypothesis.

Given the enhanced moisture convergence of the background flow over the warm tropical Indian Ocean, we now examine the evolution of transients over the equatorial region during the monsoon season of 2000. One of the most prominent global phenomenon on the subseasonal time-scale is the tropical intraseasonal oscillation (ISO). The basic features of the ISO have been documented by numerous studies; a comprehensive review of the observational aspects of the ISO has been described by Madden and Julian (1994). To a first order, the ISO consists of eastward propagating planetary-scale perturbations of atmospheric circulation with predominant wavenumbers 1 and 2. The largest amplitudes of the ISO occur over the Indian and western Pacific Oceans and the convective anomalies in this sector exhibit a slow eastward propagation having phase speed of about $5ms^{-1}$ and the dominant periods of the ISO range from 30 to 60 days. The plot in Fig.9 shows the longitude-time section of pentadal rainfall anomalies over the near-equatorial region during 2000. The rainfall anomalies were constructed by subtracting the smooth pentadal climatology from the CMAP rainfall for 2000. One can notice that the longitudinal band extending from the central Indian Ocean upto the west Pacific Ocean (70-130°E) in Fig.9 is characterized by four major wet spells during the June-September months of 2000. The first enhanced rainfall spell over the equatorial Oceans occurred during early June; the second during later half of June and early July; the third spell was a long one extending from the third week of July upto the second week of August; the fourth spell started around the second week of September and lasted about 2 weeks or so. It should be pointed out that the II, III and IV wet events over the equatorial sector approximately coincided with the three major break spells over the Indian land region. Further it is important to notice in Fig.9 that the equatorial rainfall anomalies were largely confined over the warm waters of the Indian and western Pacific Oceans; and had rather small amplitudes to the east of the dateline. Observational evidence indicate that the variability of convection associated with the ISO can be substantial over warm SST regions of tropical Indian and western Pacific Oceans (Weickmann *et al.*, 1985). Theoretical and modeling studies provide support for the intensification and slowing down of the eastward propagating equatorial waves due to the effect of increased moisture convergence (Lau and Peng, 1987, Wang,1988, Kasture *et al.*, 1991 and several others). In the light of these discussions, it is quite likely that

the intensified convection over the equatorial Indian Ocean during the 2000 monsoon season might have been generated largely from a combined influence of increased large-scale moisture convergence over the warm ocean surface and the amplification of the transient convective activity associated with the ISO.

3 Model experiments

In this section, we will describe the GCM experiments that were performed in order to assess the atmospheric response to the SST forcing during 2000. We have carried out four sets of 10-member ensemble integrations using the COLA GCM. These ensemble runs involve integrating the GCM from ten different initial conditions and provide a means for assessing the robustness of the simulated response to a given boundary forcing. The need to consider such multiple realizations arises due to fact that model simulations of the seasonal mean monsoon are affected not only by slowly varying boundary conditions like SST but also by atmospheric internal dynamics (Brankovic and Palmer, 1997, Mujumdar and Krishnan, 2001). Thus ensemble realizations obtained from the multiple runs of the GCM starting from different initial conditions enables the determination of estimates for statistical significance of the simulated anomalies. A summary of the SST boundary forcing and initial conditions used in our experiments is presented in Table.1. The ensemble runs were initiated from ten different observed initial conditions (22-31, May 2000) from NCEP. We first processed the NCEP initial conditions containing the spectral coefficients of vorticity, divergence, temperature, moisture and surface pressure so that they become compatible with the COLA T30L18 GCM. Subsequently these 10-member initial conditions were used to start the model runs in all the four experiments. In the first set (CLIM) of ensemble experiments, we use the observed monthly climatological SSTs as boundary forcing for the GCM. The boundary forcing for the second set (GL2K), is obtained by superposing the observed monthly SST anomalies of 2000 upon the monthly climatology for the global oceans. In the third set (IO2K), we superpose the monthly SST anomalies of 2000 on the climatological SST only in the Indian Ocean (40-120°E); while retaining climatological SSTs in all the other oceans. The meridional extent of the IO2K domain includes the 2000 SST anomalies for the entire Indian Ocean extending from Bay of Bengal, Arabian Sea, Tropical and Southern Indian Ocean. The idea behind the IO2K experiment is to understand exclusively the influence of the the Indian Ocean SST anomalies on the atmosphere. In the fourth experiment (NOIO), we specify climatological SST in the Indian Ocean (40-120°E) and superpose the 2000 monthly SST anomalies on the climatology in all other oceans. Unlike the IO2K case, the NOIO experiment is intended to evaluate the influence of SST anomalies in all other oceans excepting the Indian Ocean. The procedure adopted for evaluating the anomalous response to SST forcing is to compare the ensembles of the GL2K, IO2K and NOIO simulations with those of the CLIM experiment. Since the four experiments have been initiated from identical sets of ten observed initial conditions; it is possible to carry out a member-to-member comparison between the (GL2K and CLIM); (IO2K and CLIM) and (NOIO and CLIM) experiments. This approach provides a straight-forward means for assessing the simulated response to SST forcing (Mujumdar and Krishnan, 2001).

Table 1. GCM Experiments

Exp.	SST Boundary Condition	Initial Condition
CLIM-01	Observed Climatological SST	22 May 2000
CLIM-02	Observed Climatological SST	23 May 2000
CLIM-03	Observed Climatological SST	24 May 2000
CLIM-04	Observed Climatological SST	25 May 2000
CLIM-05	Observed Climatological SST	26 May 2000
CLIM-06	Observed Climatological SST	27 May 2000
CLIM-07	Observed Climatological SST	28 May 2000
CLIM-08	Observed Climatological SST	29 May 2000
CLIM-09	Observed Climatological SST	30 May 2000
CLIM-10	Observed Climatological SST	31 May 2000
GL2K-01	Observed Climatological SST +Anomalies of 2000 for global oceans	22 May 2000
GL2K-02	Observed Climatological SST +Anomalies of 2000 for global oceans	23 May 2000
GL2K-03	Observed Climatological SST +Anomalies of 2000 for global oceans	24 May 2000
GL2K-04	Observed Climatological SST +Anomalies of 2000 for global oceans	25 May 2000
GL2K-05	Observed Climatological SST +Anomalies of 2000 for global oceans	26 May 2000
GL2K-06	Observed Climatological SST +Anomalies of 2000 for global oceans	27 May 2000
GL2K-07	Observed Climatological SST +Anomalies of 2000 for global oceans	28 May 2000
GL2K-08	Observed Climatological SST +Anomalies of 2000 for global oceans	29 May 2000
GL2K-09	Observed Climatological SST +Anomalies of 2000 for global oceans	30 May 2000
GL2K-10	Observed Climatological SST +Anomalies of 2000 for global oceans	31 May 2000
IO2K-01	Observed Climatological SST +Anomalies of 2000 for Indian Ocean only	22 May 2000
IO2K-02	Observed Climatological SST +Anomalies of 2000 for Indian Ocean only	23 May 2000
IO2K-03	Observed Climatological SST +Anomalies of 2000 for Indian Ocean only	24 May 2000
IO2K-04	Observed Climatological SST +Anomalies of 2000 for Indian Ocean only	25 May 2000
IO2K-05	Observed Climatological SST +Anomalies of 2000 for Indian Ocean only	26 May 2000
IO2K-06	Observed Climatological SST +Anomalies of 2000 for Indian Ocean only	27 May 2000
IO2K-07	Observed Climatological SST +Anomalies of 2000 for Indian Ocean only	28 May 2000
IO2K-08	Observed Climatological SST +Anomalies of 2000 for Indian Ocean only	29 May 2000
IO2K-09	Observed Climatological SST +Anomalies of 2000 for Indian Ocean only	30 May 2000
IO2K-10	Observed Climatological SST +Anomalies of 2000 for Indian Ocean only	31 May 2000
NOIO-01	Observed Climatological SST +Anomalies of 2000 everywhere except Indian Ocean	22 May 2000
NOIO-02	Observed Climatological SST +Anomalies of 2000 everywhere except Indian Ocean	23 May 2000
NOIO-03	Observed Climatological SST +Anomalies of 2000 everywhere except Indian Ocean	24 May 2000
NOIO-04	Observed Climatological SST +Anomalies of 2000 everywhere except Indian Ocean	25 May 2000
NOIO-05	Observed Climatological SST +Anomalies of 2000 everywhere except Indian Ocean	26 May 2000
NOIO-06	Observed Climatological SST +Anomalies of 2000 everywhere except Indian Ocean	27 May 2000
NOIO-07	Observed Climatological SST +Anomalies of 2000 everywhere except Indian Ocean	28 May 2000
NOIO-08	Observed Climatological SST +Anomalies of 2000 everywhere except Indian Ocean	29 May 2000
NOIO-09	Observed Climatological SST +Anomalies of 2000 everywhere except Indian Ocean	30 May 2000
NOIO-10	Observed Climatological SST +Anomalies of 2000 everywhere except Indian Ocean	31 May 2000

3.1 Simulated seasonal features

a. Rainfall and moisture transport

The ensemble mean of the seasonal rainfall and moisture transport vector simulated by CLIM experiment is shown in Fig.10a. The overall spatial distribution of the monsoon precipitation is reasonably captured by the GCM; the simulated water vapor transport by the southwest monsoon winds and the cross-equatorial flow is broadly consistent with that of the NCEP reanalysis. However some of the finer details of monsoon rainfall are not as well simulated - may be partly because of the course model resolution and partly due to deficiencies in the treatment of physical processes in the GCM. For instance, the west coast rainfall maximum over India is weak and is shifted more westward as compared to the CMAP precipitation. Also the rainfall maximum over the Bay of Bengal shows a southward shift relative to the observed position. While noting such discrepancies, we must also point out that a large number of the state-of-the-art GCMs face a big challenge in accurately simulating the monsoon rainfall distribution (Gadgil and Sajani, 1998). Moreover, it is important to mention that the primary purpose of the GCM experiments is not to critically focus on the accuracy on the monsoon simulation; instead the experiments are aimed at providing an overall picture of the large-scale character of monsoon and its anomalous behavior during 2000.

We shall now examine the anomalous response to SST forcing in the GL2K experiment. For this reason, we compute the mean of the member-to-member differences between the GL2K and CLIM experiments. The statistical significance of the simulated anomalies has been evaluated by applying classical t-test (Mujumdar and Krishnan, 2001). The anomaly pattern for the GL2K run in Fig.10b, shows decreased rainfall and anomalous anticyclone over the Indian subcontinent, Arabian Sea and Bay of Bengal. The anomalous easterly flux over this region indicates a decrease in the transport of moisture into India which qualitatively agrees with the NCEP anomalies (Fig.3c). The response over the southern equatorial Indian Ocean shows increased rainfall and intensified circulation. The simulated anomalies over the Indian Ocean are more westward as compared to CMAP and NCEP anomalies. Nevertheless the north-south asymmetry of the rainfall and moisture transport anomalies are broadly consistent with the CMAP and NCEP datasets. Furthermore, the shaded area in Fig.10b suggests that the contrasting rainfall anomalies over the Indian land and oceanic regions exceed the 99% level of statistical significance.

The precipitation and moisture transport anomalies for the IO2K experiment obtained from the ensemble mean of the member-to-member difference between the IO2K and CLIM runs, are shown in Fig.10c. The anomalous response in the IO2K experiment closely resembles that of the GL2K experiment with regard to the asymmetric pattern of the rainfall and moisture transport anomalies. This indicates the dominant impact of the Indian Ocean SST anomalies, which was common to both the GL2K and IO2K runs, on the GCM simulated response. The t-test for the IO2K simulation shows that the opposite polarity of the rainfall anomalies over the Indian land and oceanic regions are statistically significant. The simulated precipitation and moisture transport anomalies in the NOIO experiment (Fig.10d) are weak and insignificant over most of the region. The small negative values of rainfall anomalies over the eastern southern Indian Ocean seem to be in response to the SST anomalies in the tropical west Pacific Ocean.

b. Monsoon Hadley circulation

The simulated overturning in the y-p plane for the CLIM experiment (Fig.11a) is qualitatively consistent with the NCEP reanalysis in capturing the monsoon Hadley cell with ascending branch to the north of 15°N and descending motion over the Southern Indian Ocean. The y-p circulation anomaly for the GL2K experiment (Fig.11b) shows a weakening of the Hadley cell characterized by anomalous sinking around 15-20°N and anomalous rising motion around 0-10°S over the tropical Indian Ocean. The circulation anomaly in GL2K experiment appears to be more pronounced than that of the NCEP reanalysis, suggestive of the rather strong sensitivity of the GCM response to SST forcing. The anomalous weakening of the monsoon Hadley in the IO2K experiment (Fig.11c) is strikingly similar to that of GL2K run. On the other hand, the changes in the monsoon Hadley cell for the NOIO experiment are almost negligible. We realize that there are differences between the model simulation and the reanalysis fields; however the encouraging point is that both the datasets are broadly consistent in indicating the asymmetric distribution of the precipitation and circulation anomalies in response to the Indian Ocean SST forcing during 2000.

3.2 Simulation of monsoon breaks

It has been recognized that the mean summer rainfall over India during a particular year is substantially influenced by the monsoon intraseasonal variability (Goswami and Ajaya Mohan, 2001). The conceptual model for the intraseasonal oscillations of the monsoon system proposed by Krishnamurti and Bhalme (1976) involves interactions among dynamics, moist-convection and cloud-radiative processes. The question that now arises is about the external influence of SST forcing on the monsoon intraseasonal oscillations. In the context of the 2000 monsoon, we shall specially examine as to how tropical Indian Ocean SST anomalies can affect monsoon breaks over India.

a. Observed break pattern

First we illustrate the spatial pattern of the observed rainfall and low-level wind anomalies associated with monsoon breaks that occurred in 2000. The plot in Fig.12a shows composites of pentadal anomalies for the three major break spells that were discussed earlier. The pattern of the negative rainfall anomaly over the Indian land region and the positive anomaly over the equatorial Indian Ocean in Fig.12a resembles the first EOF already described in Fig.6a. Such an out-of-phase pattern of convective anomalies over the two regions has been reported by previous studies (Yasunari, 1979; Sikka and Gadgil, 1980, Krishnan *et al.*, 2000). The anomalous easterlies and the anticyclonic circulation (Fig.12a) to the north indicate a weakening of the monsoon flow; while the anomalous low-level convergence over the Indian Ocean represents an intensification of the equatorial shear zone. The strengthening of the near-equatorial shear zone, commonly referred to as the Southern Hemispheric Equatorial Trough, during monsoon breaks has been well-known in the Indian meteorological literature (De, it et al., 1997). The small region of increased rainfall over Northeast India is a characteristic feature of breaks and is accompanied by a northward shift of the monsoon trough to the Himalayan foothills (Ramamurthy, 1969, Dhar *et al.*, 1984, Krishnamurthy and Shukla, 2001).

b. Simulated break pattern

We shall now examine the GCM simulation of monsoon breaks using the model outputs of daily rainfall anomalies. The anomalies were computed relative to daily rainfall normals of the model prepared by averaging the rainfall output from a large number of CLIM SST runs initiated from different initial conditions (see text of Fig.12b). The time-series of the daily normal rainfall for the GCM, averaged over the Indian region, is shown in Fig.12b. It can be seen that a large part of the monsoon rainfall in the model occurs during July and August months. The low rainfall in the beginning and end periods of the integrations are associated with model spin-up and early withdrawal of the monsoon respectively, which should not impact the thrust of this analysis (Mujumdar and Krishnan, 2001). Having prepared the daily rainfall normals and the daily anomalies for all the members of the 4 GCM experiments, we now proceed to identify the break days simulated by the GCM. The criterion we have adopted in selecting the monsoon break days is that the percentage departure of the area-averaged (70-95°E; 10-30°N) rainfall from the normal should be below 30% for atleast 5 consecutive days. In adopting the above definition, we keep in mind the broad spatial pattern of observed rainfall departures during breaks which can vary from about -25 % over a wide area of central India upto about -75 % over the drier regions of northwest India (Ramamurthy, 1969). In the next step, break days are identified for the different ensembles of CLIM, GL2K, IO2K and NOIO experiments. Based on the identified break days, we have prepared break composites of rainfall and low-level circulation anomalies for the four experiments. In calculating the composite for a given experiment (say GL2K), we determine the break anomaly patterns separately for all the 10 ensemble members and later take an average over all the break anomaly patterns.

The break anomaly composites for the CLIM, GL2K, IO2K and NOIO experiments are shown in Figs.12(c,d,e,f) respectively. The composite in the CLIM experiment shows a pattern of decreased rainfall and low-level anticyclonic anomaly over the India; the Arabian Sea and Bay of Bengal. A slight increase in the precipitation is seen to the south of the equatorial Indian Ocean. The SST boundary condition in the CLIM experiment contains only the climatologically varying component. Hence, the break composite for the CLIM experiment basically reflects the rainfall decrease resulting from atmospheric internal dynamics and does not contain the influence of SST anomalies. On the other hand, the spatial pattern of break anomalies for the GL2K and IO2K experiments include contributions both from atmospheric internal dynamics as well as the SST anomalies of 2000. We can see that the break monsoon anomalies in GL2K and IO2K appear to be more intense with a wider spread as compared to the CLIM runs. Particularly the rainfall increase over the equatorial and southern Indian Ocean and the anomalous intensification of the near-equatorial shear zone is more pronounced in the GL2K and IO2K experiments. We also recognize some of the limitations of the GL2K and IO2K simulation relative to the observed pattern of break monsoon anomaly. Especially it can be seen that the simulated rainfall anomaly over the Southern Indian Ocean is shifted more westward as compared to the observed break pattern (Fig.12a). Also the GCM does not adequately capture the larger eastward spread of the negative rainfall anomalies to the north which is seen in the observed break composite. Despite these differences, the GL2K and IO2K simulations are overall consistent with observations in indicating the reinforcement of the north-south asymmetric structure of break monsoon rainfall anomaly which is suggestive of the effect induced by the SST anomalies during 2000. The break composite for the NOIO

experiment (Fig.12f) shows negative rainfall anomalies over India and northern Bay of Bengal. The spatial extent of the negative rainfall anomaly over the Indian region is relatively small in the NOIO experiment as compared to the GL2K and IO2K experiments. Also the rainfall increase over the equatorial Indian Ocean is marginal in the NOIO experiment. Although both the CLIM and NOIO experiments make use of climatological SST in the Indian Ocean, the SST boundary condition in the NOIO case includes contribution from the 2000 SST anomalies in all other oceans as well. The consequence of such differences in the SST boundary conditions in the two experiments may be partly reflected in some of the regional differences in the break composites of the NOIO and CLIM experiments. For instance the pattern of decreased rainfall extends more westward into the Arabian Sea in the CLIM run as compared to the NOIO run. Likewise, the increased rainfall to the south of the equator appears to be shifted more westward in the CLIM case as compared to the NOIO run. Nevertheless both the CLIM and NOIO experiments share a common feature in showing a relatively weaker north-south asymmetric pattern of rainfall anomalies as compared to the GL2K and IO2K experiments.

The plot in Fig.13 shows the frequency distribution of monsoon rainfall departures simulated by the 4 sets of ensemble experiments. In computing the above statistics, we have utilized the outputs of daily rainfall from the different ensemble members of the four experiments. By organizing the monsoon rainfall departures into categories (or classes), we have determined the number of days belonging to each category. The four curves in Fig.13 is averages of distributions from the 10 ensemble realizations. It can be seen from Fig.13 that the distribution for the CLIM experiment is centered around zero. The shape of the CLIM distribution on either side of the maximum is nearly same. The GL2K and IO2K distributions have maxima centered around -45 % and their shapes are clearly skewed towards the negative side. Note that the maximum frequency of the GL2K and IO2K distributions are about 20 and 24 days respectively. This suggests that on an average, the GL2K and IO2K experiments showed atleast 20 days (within a season) during which the rainfall was deficient by -45 %. The NOIO distribution shows maximum around -10 %; but the skewness is not clearly apparent in the NOIO case. Moreover it may be noted that the shape of the NOIO curve is more or less similar for both the positive and negative departures. Thus the frequency curves suggest that the intraseasonal variations of monsoon rainfall in the GL2K and IO2K runs were significantly inclined towards break spells as compared to the CLIM and NOIO cases. We have also confirmed that the total count of break days during the monsoon season were generally more in number in the GL2K and IO2K runs relative to the CLIM and NOIO ensembles. These results offer justification for the amplification and sustenance of break monsoon condition in the presence of warm Indian Ocean SST anomalies as in 2000.

4 Intraseasonal convection and Indian Ocean SST: Extended analysis

Prompted by the results of the 2000 case-study, we now extend our analysis of observed datasets for other years as well. The issue here is to explore from the past observed records the signatures of the Indian Ocean SST forcing in contributing to the out-of-phase behavior of intraseasonal variability over the Indian Ocean and the monsoon region. The daily time-series

of All India rainfall during the summer season provides a reliable measure of intraseasonal variations of monsoon activity over the subcontinent. For information about convection over the Indian Ocean, we rely on the daily observed OLR measured from Advanced Very High Resolution Radiometers aboard the NOAA spacecraft (Gruber and Krueger, 1984). Deep convection in the tropics is characterized by low cloud-top temperatures and small OLR values. On the other hand, regions having high OLR values indicate scarcity or absence of cloud cover. Thus OLR averaged over a wide area (70-100°E; 10°S-EQ) over the tropical Indian Ocean is a good proxy for convection over that region. The time-series of daily OLR and the daily All India rainfall are both available for 22-years (1979-2000).

The histogram in Fig.14a shows the correlation coefficient (CC) between the time-series of daily rainfall over India and the daily OLR over the equatorial and Southern Indian Ocean. For each of 22 years (1979-2000), we compute the CC between the two daily time-series for 93 days (15 Jun - 15 Sep) during the core monsoon season. The first and last 15 days are not considered because of variations in the onset and withdrawal of monsoon during different years. It is to be noted that the CCs are positive for all the years; although there are variations in the magnitude of the CCs from one year to another. A positive CC implies that an increase in the monsoon rainfall over India tends to be accompanied by increased OLR (decreased convection) over the equatorial Indian Ocean; conversely a decrease in the monsoon rainfall over India tends to be accompanied by decreased OLR (increased convection) over the Indian Ocean. This out-of-phase intraseasonal variability is consistent with the findings of earlier studies (Yasunari, 1979; Sikka and Gadgil, 1980; Krishnan *et al.*, 2000). Here it is important to recognize that higher CCs only suggest a close relationship of the intraseasonal fluctuations between the two regions. However high CCs alone are not enough for inferring about the nature of the seasonal anomalies. For instance, it can be seen that the CCs were large during 1996 and 1998; yet the seasonal monsoon rainfall turned out to be nearly normal in these two years (Fig.14b). Our main concern now is to identify those years for which the seasonal monsoon rainfall departures were significantly large; and were also associated with significant correlation between the intraseasonal variability over the Indian land and oceanic areas. In the context of the present study, we shall particularly focus on deficient monsoon rainfall years for which *the negative departures of the seasonal rainfall exceeded atleast 5 % of the normal*; while at the same time *the CCs between the daily All India rainfall and the daily OLR over the equatorial and southern Indian Ocean exceeded 99 % significance level.* From Figs.14(a,b), one can identify 5 monsoon seasons (1979, 1986, 1987, 1995, 2000) that satisfy the above objective criteria. Out of the five cases, the three monsoon seasons during (1979, 1986, 1987) in fact turned out be severe droughts (Sikka, 1999). The major breaks that occurred during (1979, 1986, 1987, 1995) were characterized by either prolonged break spells or multiple spells within a season or a combination of both (Krishnan *et al.*, 2000). Thus the selected cases essentially represent weak monsoon years that were dominated by strong intraseasonal break spells.

The plot of the CMAP seasonal rainfall anomaly in Fig.15a is a composite of the five identified cases. The anomaly pattern shows a patch of increased rainfall over the equatorial and southern tropical Indian Ocean extending eastward from about 70°E into the Sumatran coast and even beyond. To the north, one can notice wide-spread decrease of monsoon rainfall over the plains of India. The rainfall increase seen over northeast India during deficient

monsoon seasons is consistent with the findings of Krishnamurthy and Shukla (2001). The composite plot of the observed SST anomalies (Fig.15b) shows warmer than normal SSTs in the equatorial and southern Indian Ocean stretching across 60-105 °E. The meridional gradient of the SST anomaly decreases as we progress from the equatorial Indian ocean towards the northern Arabian Sea. The maximum value of the composited anomaly is about 0.8°C which occurs around 70°E. The corroborative evidence from the above composite analysis suggests that the existence of warm SST anomalies in the tropical Indian Ocean, during several instances in the past, might have favored the enhancement of the near-equatorial intraseasonal convective activity; which in turn amplified the break condition over India and provided a means for sustaining the seasonal rainfall anomalies in the region. This result is supported by the statistical analysis of Annamalai *et al.,* (1999) and the GCM simulations of Mujumdar and Krishnan (2001) which indicate that the monsoon activity tends to be generally skewed towards break phases in the presence of warm SST conditions in the tropical Indian and Pacific Oceans.

This paper has largely alluded to the issue of increased convection over the equatorial Indian Ocean and its consequences on the monsoon circulation. There is evidence that some of the strong monsoon years like (1961, 1994) have coincided with SST cooling events occurring to the west of the Sumatran coast in the southeastern Indian Ocean (Saji *et al.*, 1999, Behera *et al.*, 1999). It has been suggested by Behera *et al.,* (1999), that evaporative cooling is one of key processes that can maintain cold SST anomalies off the Sumatran coast; while the enhanced moisture transport from this region can be important for sustaining the strong monsoon convection over the subcontinent. Recent studies have also drawn attention to the possibility of atmosphere-ocean coupling in the tropical Indian Ocean which is analogous to the Pacific ENSO (Webster *et al.*, 1999, Saji *et al.*, 1999). These studies suggest that the coupling mechanism gives rise to an east-west dipole pattern of negative (positive) SST anomalies and decreased (increased) precipitation over the eastern (western) tropical Indian Ocean (Webster *et al.*, 1999, Saji *et al.*, 1999). It will be useful to understand the possible implications of such SST patterns in affecting the atmospheric convection over the equatorial Indian Ocean and the monsoon region.

5 Concluding remarks

Regional aspects of convection variability over the monsoon and the Indian Ocean area and its association with the local SST forcing have not been fully understood yet. The circumstances that prevailed in the summer of 2000 provided an extraordinary opportunity to focus on some of these issues. During this season, the rainfall over the subcontinent was significantly suppressed; on the other hand the equatorial and southern Indian Ocean was characterized by enhanced atmospheric convection overlying the warm ocean surface. The dynamical fields revealed weakening of the monsoon Hadley cell; while increased moisture convergence and anomalous ascending motions occurred over the equatorial and southern tropical Indian Ocean. These large-scale anomalous features were accompanied by coherent intraseasonal fluctuations of regional convection. The subseasonal variability was dominated by prolonged breaks in the monsoon rainfall over the plains of India; and enhanced convective activity over

the equatorial Indian Ocean. The spatial structure of the leading EOF component of intraseasonal rainfall variability exhibited a strikingly asymmetric north-south pattern of decreased precipitation over the Indian landmass, northern Arabian Sea, and the Bay of Bengal; but increased precipitation over the equatorial and southern Indian Ocean. This first PC/EOF component explained about 21 % of the total rainfall variance during 2000. Further, the timing of the monsoon breaks over India was found to match well with the time-series of the leading PC. These results confirm that the sustenance of the subseasonal convective activity over the region of the southern equatorial trough was one of the pivotal factors that altered the monsoon large-scale circulation and rainfall distribution during 2000.

The GCM simulations for the GL2K and IO2K cases, which included the effect of the 2000 Indian Ocean SST anomalies in the boundary condition, relative to the CLIM experiment were consistent in capturing the anomalous weakening of the monsoon Hadley cell and the associated moisture transport anomalies. These circulation changes were qualitatively reflected in the rainfall simulations of the GL2K and IO2K experiments which showed a significant decrease of monsoon precipitation over India, northern Arabian Sea and the Bay of Bengal; and increased precipitation over the equatorial oceanic region. The GCM results also yielded consistent support for the reinforcement of the break monsoon pattern of rainfall anomaly in response to the forcing by the warm Indian Ocean SSTs in the GL2K and IO2K experiments. Encouraged by the findings of the 2000 case-study, we have further extended the analysis of the observed records over a 22-year period (1979-2000). Evidence from this diagnosis illustrates that the out-of-phase pattern of the regional intraseasonal convective anomalies seems to have amplified in the presence of warm Indian Ocean SST anomalies during several weak monsoon years in the past. Further studies will be required in order to acquire insight into the details of the dynamical and thermodynamical processes that couple SST, convection and large-scale circulation over the Indian Ocean and the monsoon region.

Acknowledgements

The authors thank the Director, Indian Institute of Tropical Meteorology, Pune, for providing the necessary facilities to carry out this work. We acknowledge our thanks to IITM, IMD, NCEP, NOAA, CPC, CDC for making available to us the various datasets. We are grateful to Drs.J.Shukla and Mike Fennessy for providing the COLA GCM. Thanks are due to Drs.Rupa Kumar and Pattnaik for scientific inputs; Dr.Krishna Kumar for his comments on a draft version; Mr.S.P.Gharge and Mr.K.D.Barne for technical assistance.

6 References

Annamalai,H., J.M.Slingo, K.R.Sperber and K.Hodges, 1999: The mean evolution and variability of the Asian summer monsoon: Comparison of ECMWF and NCEP-NCAR Reanalysis. *Mon. Wea. Rev.*, **127**, 1157-1186.

Behera,S.K., R.Krishnan and T.Yamagata, 1999: Unusual ocean-atmosphere conditions in the tropical Indian Ocean during 1994. *Geoph. Res.Letters.*, **26**, 19, 3001-3004.

Brankovic, C., and T.N.Palmer, 1997: Atmospheric seasonal predictability and estimates of ensemble size. *Mon.Wea.Rev.*, **125**, 859-874.

Cadet,D. and G.Reverdin, 1981: Water vapour transport over the Indian ocean during summer. *Tellus*, **33**, 476-486.

Chandrasekar, A., and A. Kitoh, 1998: Impact of localized sea surface temperature anomalies over the equatorial Indian Ocean on the Indian summer monsoon. *J.Meteor.Soc. Japan*, **76**, 6, 841-853.

Chen,T.C., 1985: Global water vapour flux and maintenance during FGGE. *Mon.Wea.Rev.*, **113**, 1801-1819.

Dakshinamurti, J., and R.N.Keshavamurty, 1976: On oscillation of period around one month in the Indian summer monsoon. *Indian J.Meteor. Geophys.*, **27**, 201-203.

Dhar, O.N., M.K.Soman and S.S.Mulye, 1984: Rainfall over the southern slopes of the Himalayas and the adjoining plains during breaks in the monsoon. *J. Climatology*, **4**, 671-676.

Fennessy, M.J., J.L. Kinter, B. Kirtman, L. Marx, S. Nigam, E. Schneider, J. Shukla, A. Vernekar, Y. Xue and J. Zhou 1994: The simulated Indian monsoon: A GCM sensitivity study. *J. Clim.*, **7**, 33-43.

Gadgil,S., P.V.Joseph and N.V.Joshi, 1984: Ocean-atmosphere coupling over monsoon region *Nature*, **312**, 141-143.

Gadgil,S., and S.Sajani, 1998: Monsoon precipitation in the AMIP runs. *Clim Dyn.*, **14** 659-689.

Goswami, B.N., and Ajaya Mohan, 2001: Intraseasonal oscillation and interannual variabilit of the Indian summer monsoon. *J. Clim*, **14**, 1180-1198.

Graham,N.E., and T.P.Barnett, 1987: Sea surface temperature, surface wind divergence an convection over tropical oceans. *Science*, **238**, 657-659.

Gruber,A., and A.F.Krueger, 1984: The status of the NOAA outgoing longwave radiatio dataset. *Bull. Amer. Meteor. Soc.*, **65**, 958-962.

G. White, J. Woollen, [illegible] W. Collins, W. Duane, L. Gandin, M. Iredell, S. Saha, C. Ropelewski, J. Wang, A. Leetmaa, R. Raynolds, Jenne Roy and Dennis Joseph, 1996: The NCEP/NCAR 40-Year Reanalysis Project. *Bull. Amer. Meteor. Soc.*, **77**, 437-471.

Kasture, S.V., V.Satyan and R.N.Keshavamurty, 1991: A model study of the 30-50 day oscillation in the tropical atmosphere. **Mausam**, **42**, 241-248.

Kinter III, D.G. DeWitt, P.A. Dirmeyer, M.J. Fennessy, B.P. Kirtman, L. Marx, E.K. Schneider, J. Shukla and D. Straus, 1997: The COLA Atmosphere-biosphere general circulation model. Volume 1: Formulation, *COLA Technical Report*, **51**, Available from COLA, 4041 Power Mill Road, Suite 302, Calverton, MD 20705, USA).

Kirtman, B.P., and J.Shukla, 2000: Influence of the Indian summer monsoon on ENSO. *Q. R. Roy. Meteorol. Soc.*, **126**, 213-239.

Krishnamurti, T.N., 1985: Summer Monsoon Experiment: A review, *Mon.Wea.Rev.*, **113**, 1590-1626.

Krishnamurti, T.N., 1986: Monsoon Models, Monsoons, Eds. J.S.Fein and P.L.Stephens, John Wiley and Sons, 467-522.

Krishnamurti,T.N., and H.H.Bhalme, 1976: Oscillation of a monsoon system. Part I : Observational aspects. *J.Atmos. Sci.*, **33**, 1937-1954.

Krishnamurti,T.N., and D.Subrahmanyam, 1982: The 30-50 day mode at 850 mb during MONEX. *J. Atmos. Sci.*, **39**, 2088-2095.

Krishnamurthy, V., and J. Shukla, 2000: Intraseasonal and interannual variability of rainfall over India *J.Clim*, **13**, 4366-4377.

Krishnan,R., 1998: Interannual variability of water vapour flux over the Indian summer monsoon region as revealed from the NCEP/NCAR reanalysis (NNRA). WCRP-104, WMO /TD-No.876, 340-343. Proc. First WCRP International Conference on Reanalysis, Maryland, USA, 1997.

Krishnan.,R., C.Venkatesan and R.N.Keshavamurty, 1998: Dynamics of upper tropospheric stationary wave anomalies induced by ENSO during the northern summer: A GCM study. *Proc.Indian Acad.Sci. (Earth Planet. Sci.)*, **107**, No. 1, 65-90.

Krishnan,R., C.Zhang and M.Sugi, 2000: Dynamics of breaks in the Indian summer monsoon. *J.Atmos.Sci.*, **57**, 1354-1372.

Lau,K.-M., and L.Peng, 1987: Origin of low frequency (intraseasonal) oscillations in the tropical atmosphere. Part I: The basic theory. *J.Atmos.Sci.*, **44**, 950-972.

Lindzen, R.S., and S. Nigam, 1987: On the role of sea surface temperature gradients in forcing low level winds and convergence in the tropics. *J.Atmos.Sci.*, **44**, 2418-2436.

Madden,R.A., and P.R.Julian, 1994: Observations of the 40-50-day tropical oscillations - A review. *Mon. Wea. Rev.*, **122**, 814-837.

Mujumdar M., and R. Krishnan, 2001: Ensemble GCM simulation of the contrasting Indian summer monsoons of 1987 and 1988. *IITM Res. Rep.*, **89** ((Available from Indian Institute of Tropical Meteorology, Pune-411 008, India).

Palmer,T.N., C.Brankovic, P.Viterbo and M.J. Miller, 1992: Modelling interannual variations of summer monsoons, *J.Clim*, **5**, 399-417.

Pant, G.B., and B. Parthasarathy, 1981: Some aspects of an association between the Southern Oscillation and Indian summer monsoons. *Arch. Meteor. Geophys., Biokl.*, **B29**, 245-252.

Parthasarathy,B., A.A.Munot and D.R.Kothawale, 1995: Monthly and seasonal rainfall series for All-India homogenous regions and meteorological sub-divisions 1871-1994. *Res. Report RR-065, Indian Institute of Tropical Meteorology, Pune, India.*

Rao,G.V., and H.M.E.Van de Boogard, 1981: Structure of the somali jet deduced from Aerial observations taken during June-July 1977. Monsoon Dynamics. Ed. R.P.Pearce and J.Lighthill, Cambridge University Press, 321-331.

Rasmusson, E.M., and T.H. Carpenter, 1983: The relationship between eastern equatorial Pacific sea surface temperature and rainfall over India and Sri Lanka.*Mon. Wea. Rev.*, **111**, 517-528.

Reynolds, R.W., and T.M.Smith, 1994: Improved global sea surface temperature analyses using optimum interpolation. *J.Clim*, **7**, 929-948.

Saha,K.R., and S.N.Bavadekar, 1973: Water vapour budget and precipitation over the Arabian sea during the northern summer. Q.J.R. Meteorol. Soc., **99**, 273-278.

Saji,N.H., B.N.Goswami, P.N.Vinayachandran ad T.Yamagata, 1999: A dipole mode in the tropical Indian Ocean. *Nature*, **401**, 360-363.

Sikka,D.R., 1999: Monsoon drought in India. Joint COLA/CARE Technical Report No.2, 1-243. Center for Ocean-Land-Atmosphere Studies and Center for the Application of Research on the Environment, USA.

Shukla,J., 1975: Effects of Arabian sea surface temperature anomaly on Indian summer monsoon: A numerical experiment with the GFDL model. *J.Atmos.Sci.*, **32**, 503-511.

Shukla, J., and D.A. Paolino, 1983: The Southern Oscillation and long range forecasting of the summer monsoon rainfall over India. *Mon.Wea.Rev.*, **111**, 1830-1837.

Sikka, D.R., and S. Gadgil, 1980: On the maximum cloud zone and the ITCZ over Indian longitudes during the southwest monsoon. *Mon. Wea. Rev.*, **108**, 1840-1853.

Smith,T.M., and R.W. Reynolds, 1998: A high-resolution global surface temperature climatology for the 1961-90 base period. *J.Climate*, **11**, 3320-3323.

Wang, B., 1988: Dynamics of tropical low-frequency waves: An analysis of the moist Kelvin wave. *J.Atmos.Sci.*, **45**, 2051-2065.

Washington, W.M., R.M. Charvin and G.V. Rao, 1977: Effects of a variety of Indian Ocean surface temperature anomaly patterns on the summer monsoon circulation: Experiments with the NCAR general circulation model. *Pageoph*, **115**, 1335-1356.

Webster,P.J., J.P.Loschnigg, A.M.Moore and R.R.Leben, 1999: Coupled ocean-atmosphere dynamics in the Indian Ocean during 1997-98. *Nature*, **401**, 356-359.

Weickmann,K.M., G.R.Lussky, and J.E.Kutzbach, 1985: Intraseasonal (30-60 day) fluctuations of outgoing longwave radiation and 250 mb streamfunction during northern winter. *Mon.Wea.Rev.*, **113**, 941-961.

Xie,P., and P.Arkin, 1997: Global precipitation: A 17-year monthly precipitation based on gauge observations, satellite estimates and numerical model outputs. *Bull. Amer.Met. Soc.*, **78**, 2539-2558.

Yanai,M., C.Li and Z.Song, 1992: Seasonal heating of the Tibetan plateau and its effects on the evolution of the Asian summer monsoon, J. Met. Soc. Japan, *70*, 319-351.

Yasunari, T., 1979: Cloudiness fluctuations associated with the northern hemisphere summer monsoon. *J. Meteor. Soc. Japan*, **57**, 227-242.

Zhang,C., 1993: Large-scale variability of deep convection in relation to sea surface temperature in the tropics. *J. Climate*, **6**, 1898-1913.

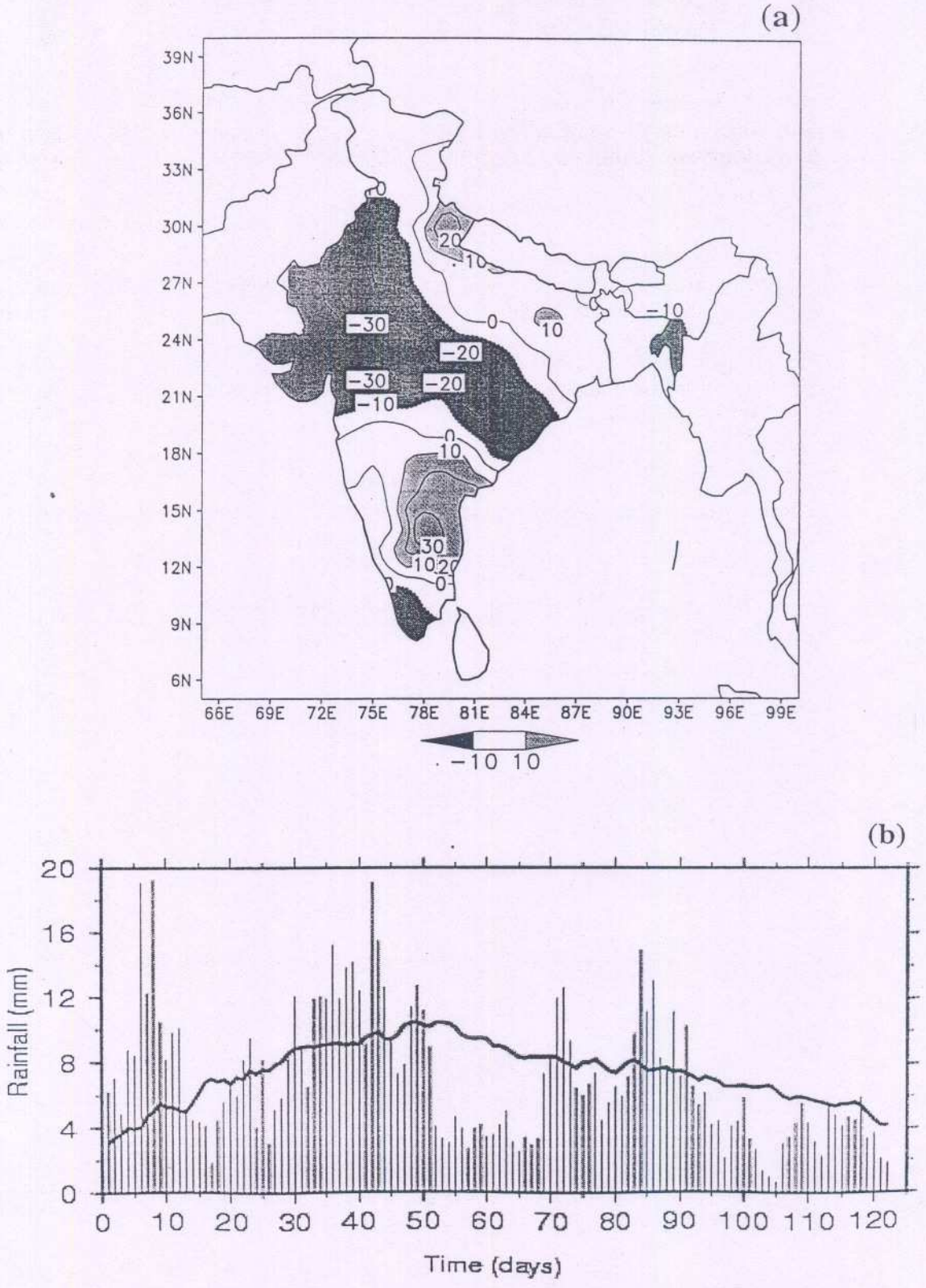

Fig.1. (a) The anomalies of the June-September (JJAS) rainfall (% departure from normal) over India during 2000 based on rainguage observations over Indian stations (http://www.tropmet.res.in). The anomalies are obtained by subtracting the long-term climatological normals over different stations. The magnitude of negative departures associated with severe drought conditions over northwest and central India (Rajasthan, Saurashtra and Kutch, Gujarat and Madhya Pradesh) exceed more than 25 %. Only very small pockets such as East Peninsular India and the hills of West Uttar Pradesh received slightly above normal rainfall. (b) Bar graph showing the daily All India Rainfall (mm) for 2000 (01 June to 30 September). The solid line is the daily climatological normal.

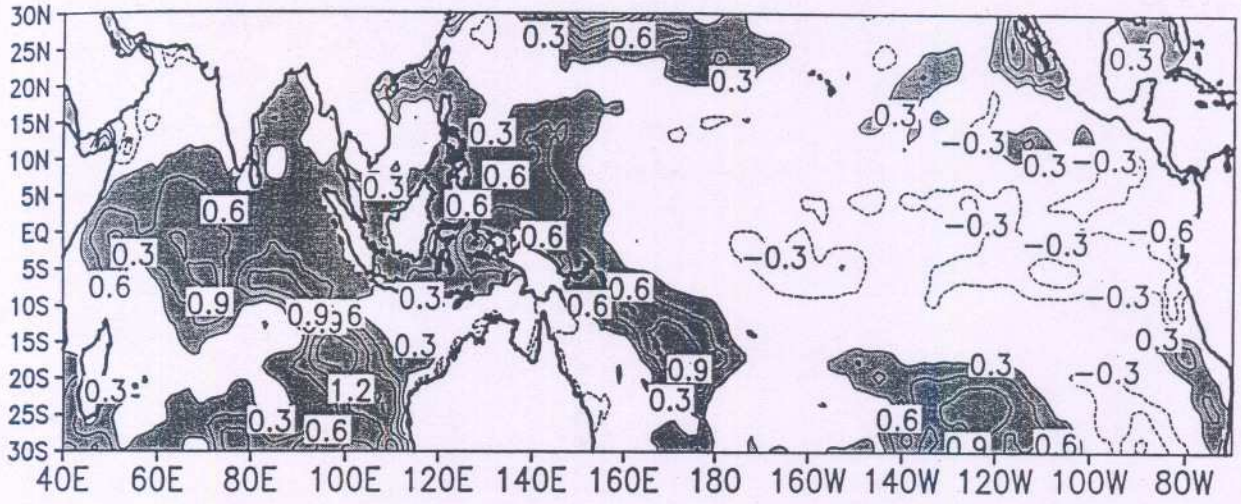

Fig.2 The observed SST (°C) anomaly for JJAS 2000 from the monthly Optimum Interpolated SST (OISST) dataset. Anomalies are with respect to the OISST climatology (Smith and Reynolds, 1998) for the base period (1961-90).

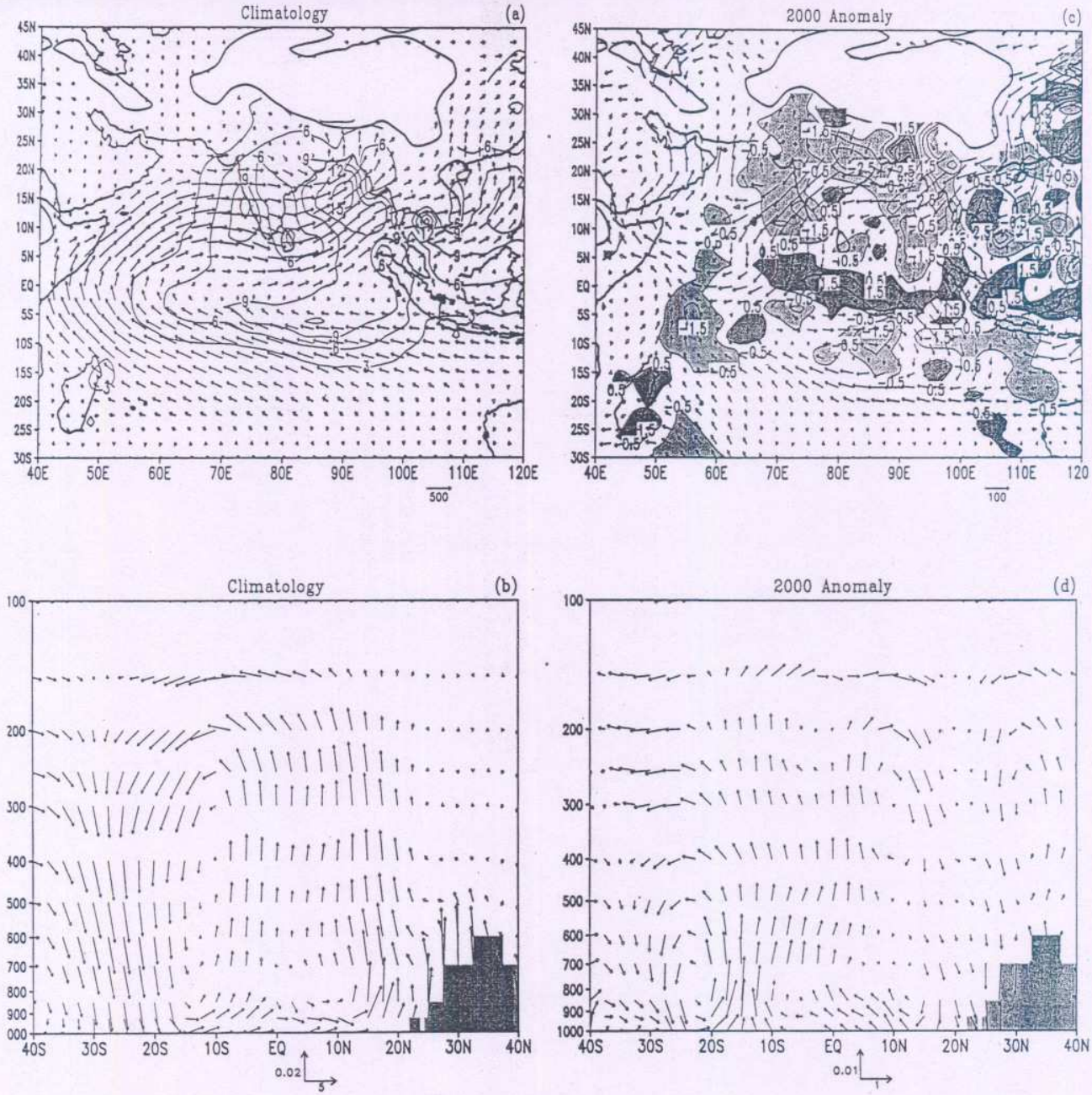

Fig.3. (a) The JJAS climatological distribution of observed rainfall (contour interval 3 mm day^{-1}) and watervapor transport vector $\vec{Q}$ (Units: Kgm $^{-1}$s^{-1}) ; $\vec{Q} = \frac{1}{g}\int_{P_u}^{P_s} q\vec{V}\, dP$ where g is the acceleration due to gravity and q is the specific humidity; P_u is 300 hPa and P_s is the surface pressure over a given geographical location. The rainfall is from the CMAP dataset; and $\vec{Q}$ is computed from NCEP reanalysis dataset. The orographic mask is shaded. (b) The JJAS climatological monsoon Hadley cell shown by the cross-section of meridional and vertical wind components averaged longitudinally between 50°-100 °E. The vertical velocity (in pressure co-ordinate hPa s^{-1}) is taken with negative sign. (c) Same as Fig.3a except for 2000 anomalies. The contour interval for rainfall anomaly is 1 mm day^{-1}. (d) Same as Fig.3b except for 2000 anomalies.

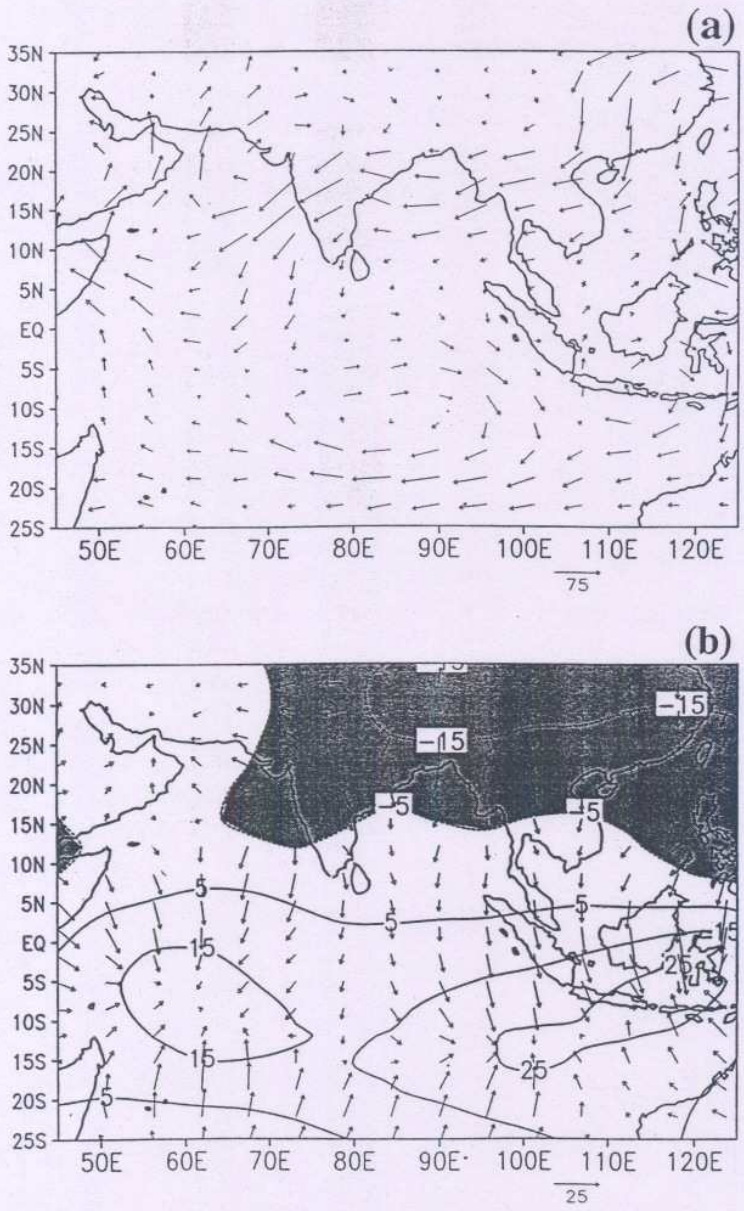

Fig.4. Anomalies for JJAS 2000 **(a)** Rotational component of water vapour transport vector $\vec{Q}_\psi$ (Units: $Kgm^{-1}s^{-1}$) **(b)** Potential function (χ_Q) (contour interval $10x10^6 Kgs^{-1}$) and divergent component of water vapour transport vector $\vec{Q}_\chi$ ($Kgm^{-1}s^{-1}$). The rotational part is given by $\vec{Q}_\psi = \hat{k} \times \nabla\psi_Q$ and the divergent part by $\vec{Q}_\chi = \nabla\chi_Q$. Here the stream function (ψ_Q) and the potential function (χ_Q) are such that $\nabla.\vec{Q}_\psi = 0$ and $\hat{k}.(\nabla \times \vec{Q}_\chi) = 0$.

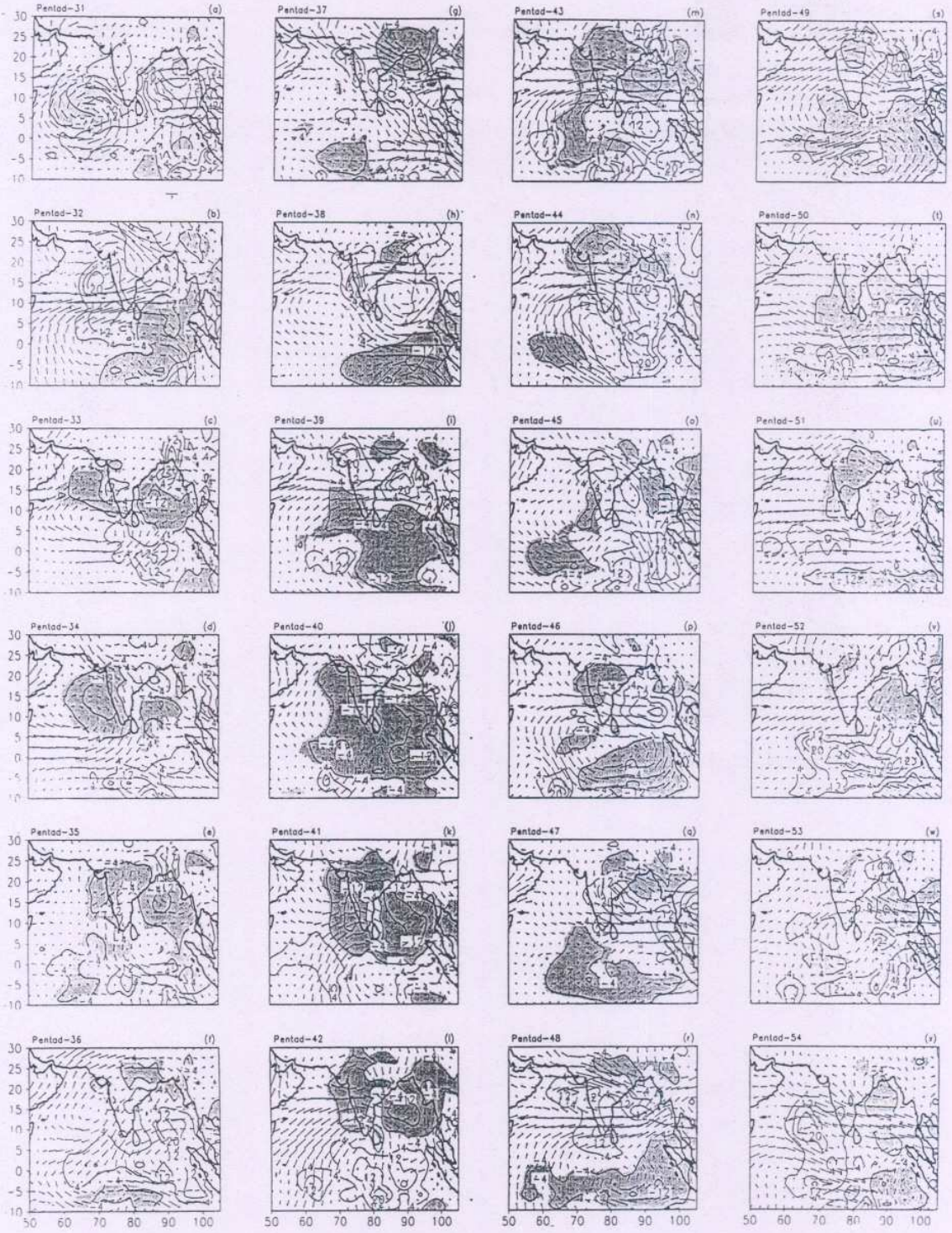

Fig.5(a-x) Pentadal anomalies of CMAP rainfall (mm day^{-1})and 850 hPa winds (ms^{-1} from NCEP reanalysis during monsoon 2000. Pentad 31 is centered around 1 June, 2000. The contour interval for the rainfall anomaly is 4 mm day^{-1}.

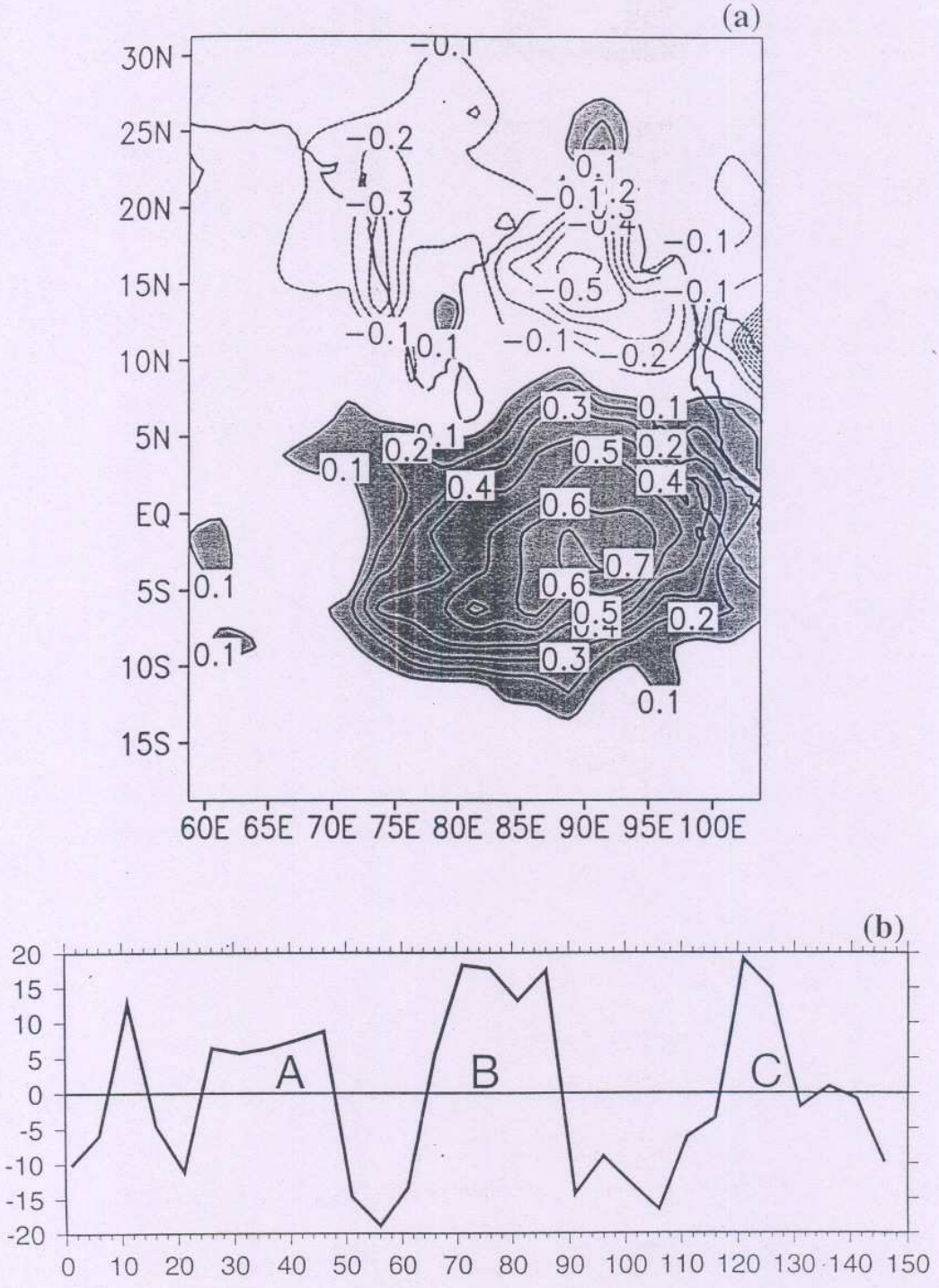

Fig.6. (a) The spatial distribution of the first EOF component of rainfall calculated from the pentadal rainfall data for monsoon 2000. Note that the intraseasonal variability is dominated by the pattern of rainfall anomaly having opposite polarities over the Indian landmass and the tropical Indian Ocean. (b) The time-series of the first PC. The symbols (A, B, C) roughly coincide with the timing of the three major break spells during 2000.

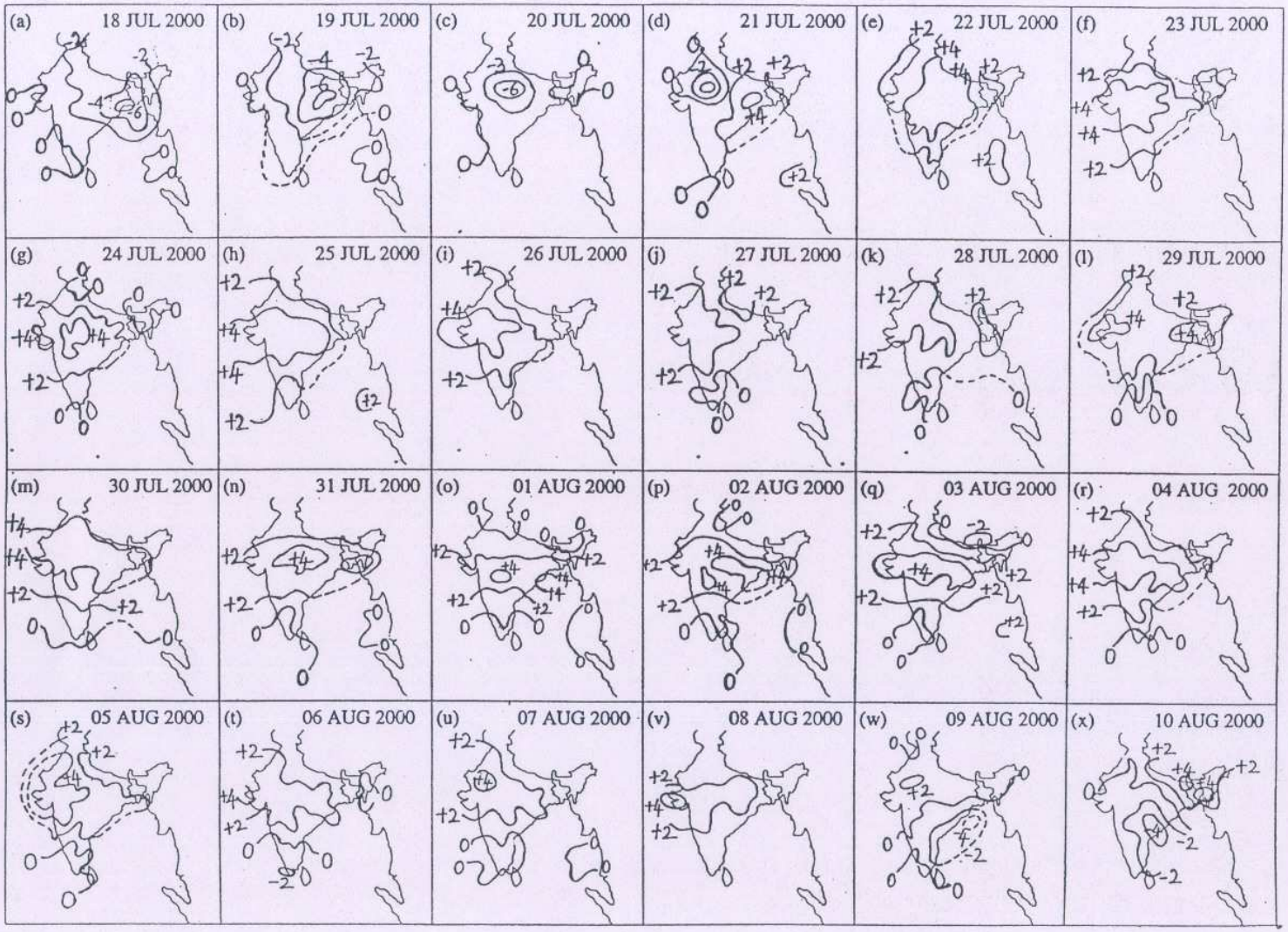

Fig.7(a-x) The daily pressure departure (hPa) maps from IMD for the period (18 July - 10 August) 2000, depicting the evolution of the second major break spell that lasted for over 18 days. The pressure departure maps have been electronically scanned from the IMD daily charts.

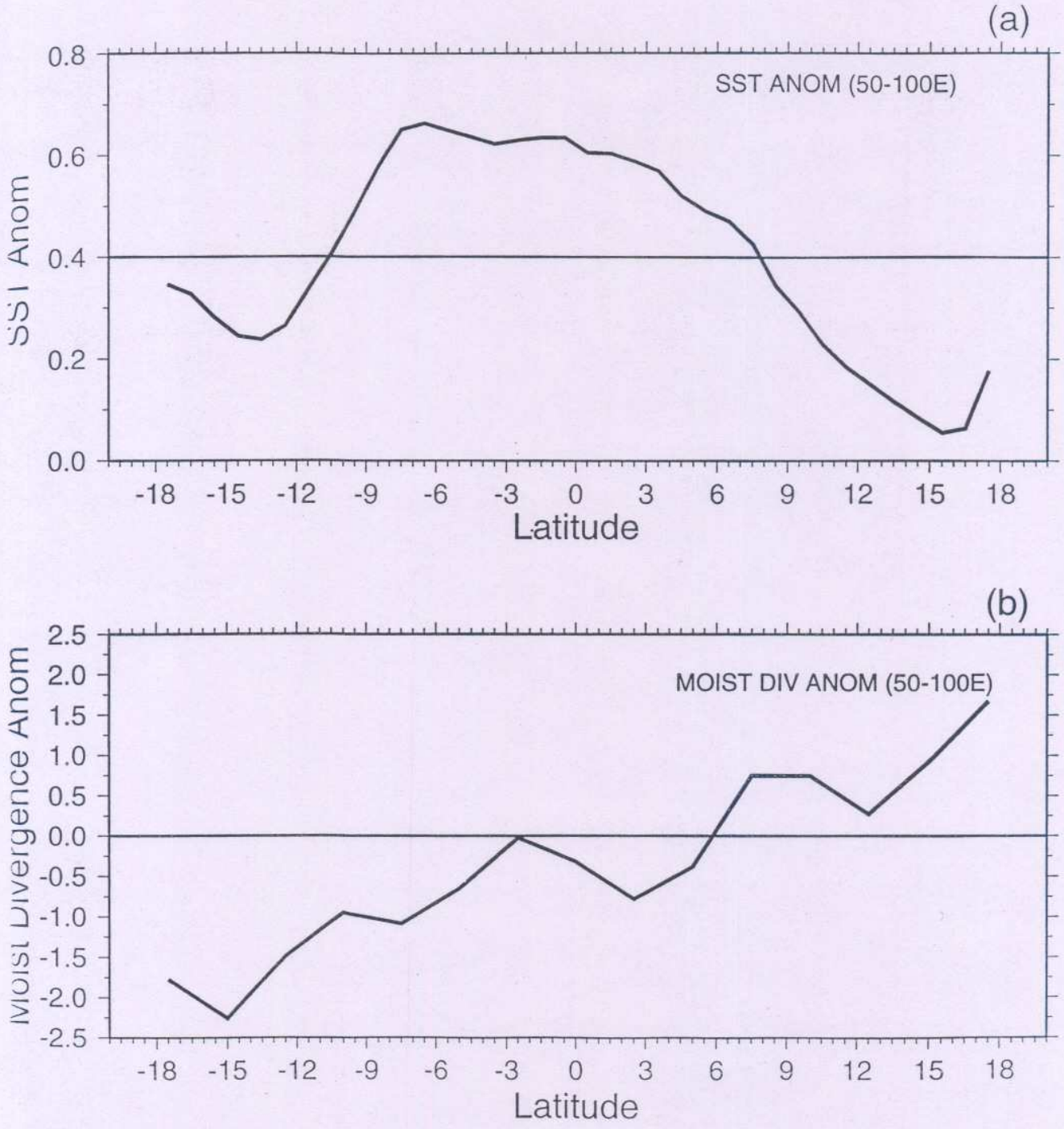

Fig.8 The latitudinal variation of (a) SST anomaly (°C) (b) Moisture divergence anomaly ($1.0x10^{-6}s^{-1}$) for JJAS 2000. The SST and moisture divergence anomalies were averaged zonally between (50°-100°E).

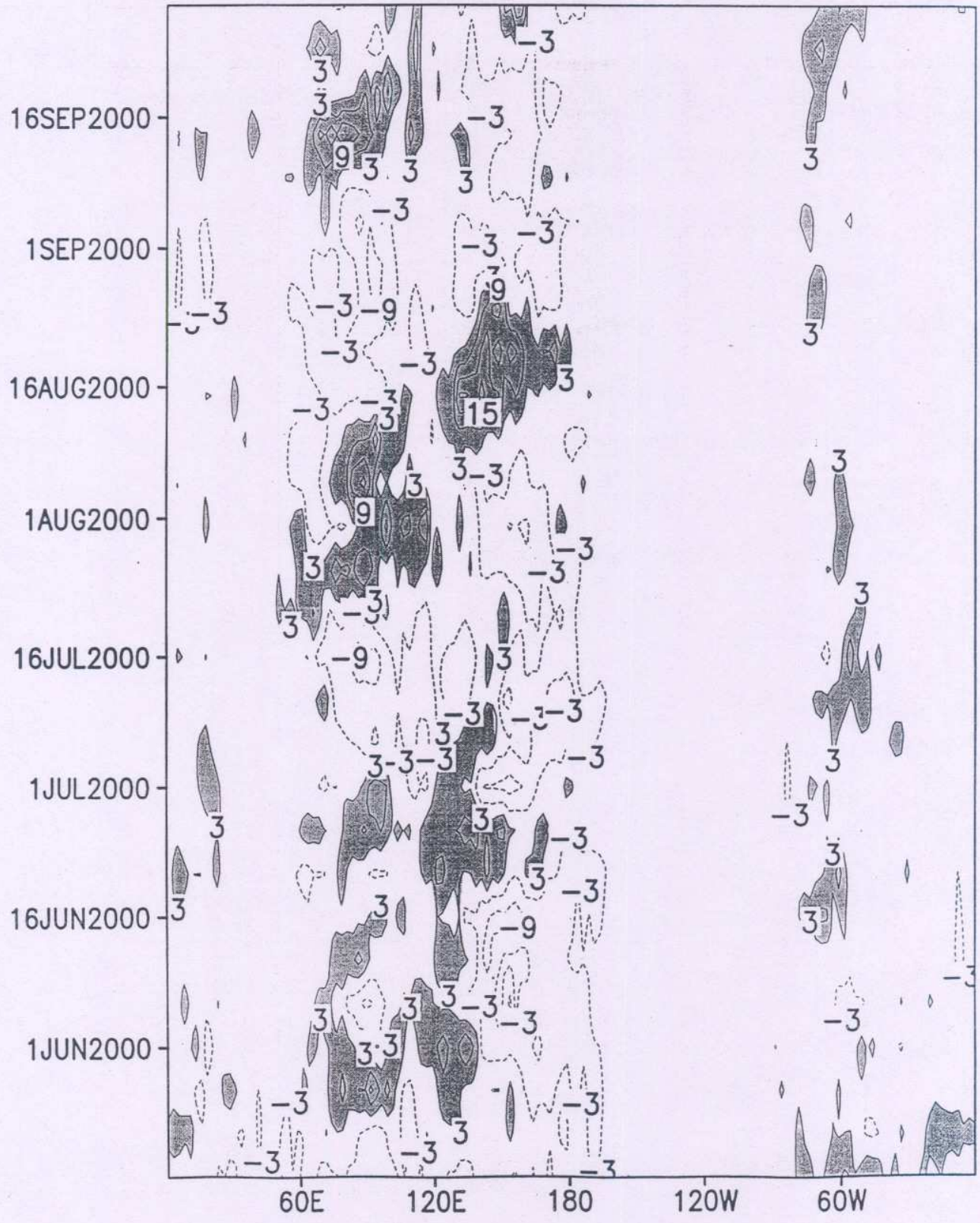

Fig.9. The longitudinal variation of the CMAP pentadal rainfall (mm day^{-1}) anomalies during 2000. The anomalies were averaged between 5°S - 5°N. Note that the equatorial intraseasonal oscillations are strongly confined over the Indian Ocean and the West Pacific sector.

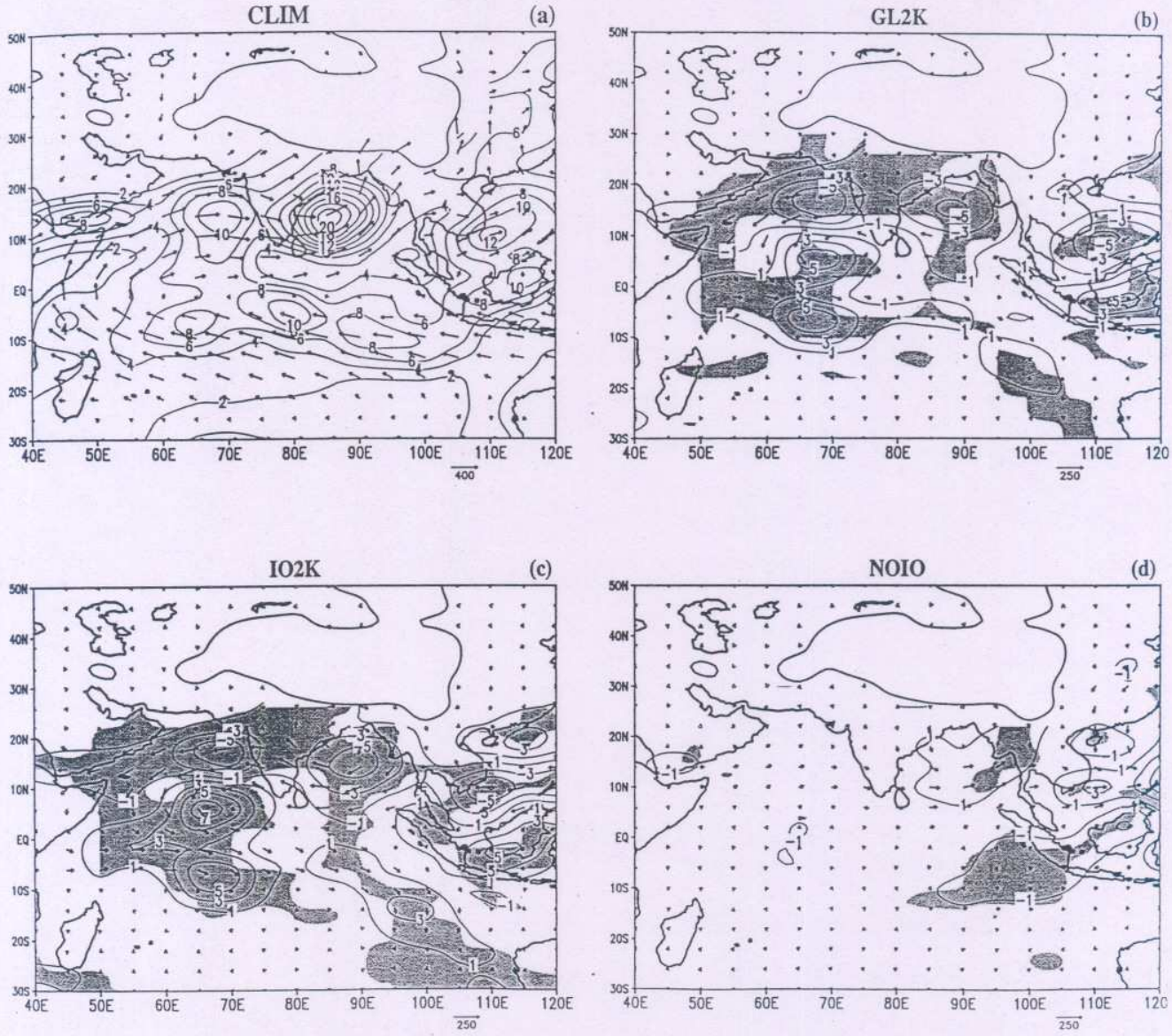

Fig.10. (a) The GCM simulated JJAS rainfall (contour interval 3 mm day^{-1}) and $\vec{Q}$ (Units: Kgm $^{-1}$s^{-1}) for the CLIM experiment. The fields shown are average of all the 10 ensemble realizations. (b) Same as (a) except for the GL2K anomalies. (c) Same as (a) except for the IO2K anomalies. (d) Same as (a) except for the NOIO anomalies. The anomalies in (b,c,d) are obtained by taking averages of the member-to-member differences for (GL2K and CLIM), (IO2K and CLIM) and (NOIO and CLIM) respectively. The shaded areas in (b,c,d) correspond to areas over which the simulated rainfall anomaly exceeded the 99 % significance level computed from a t-test.

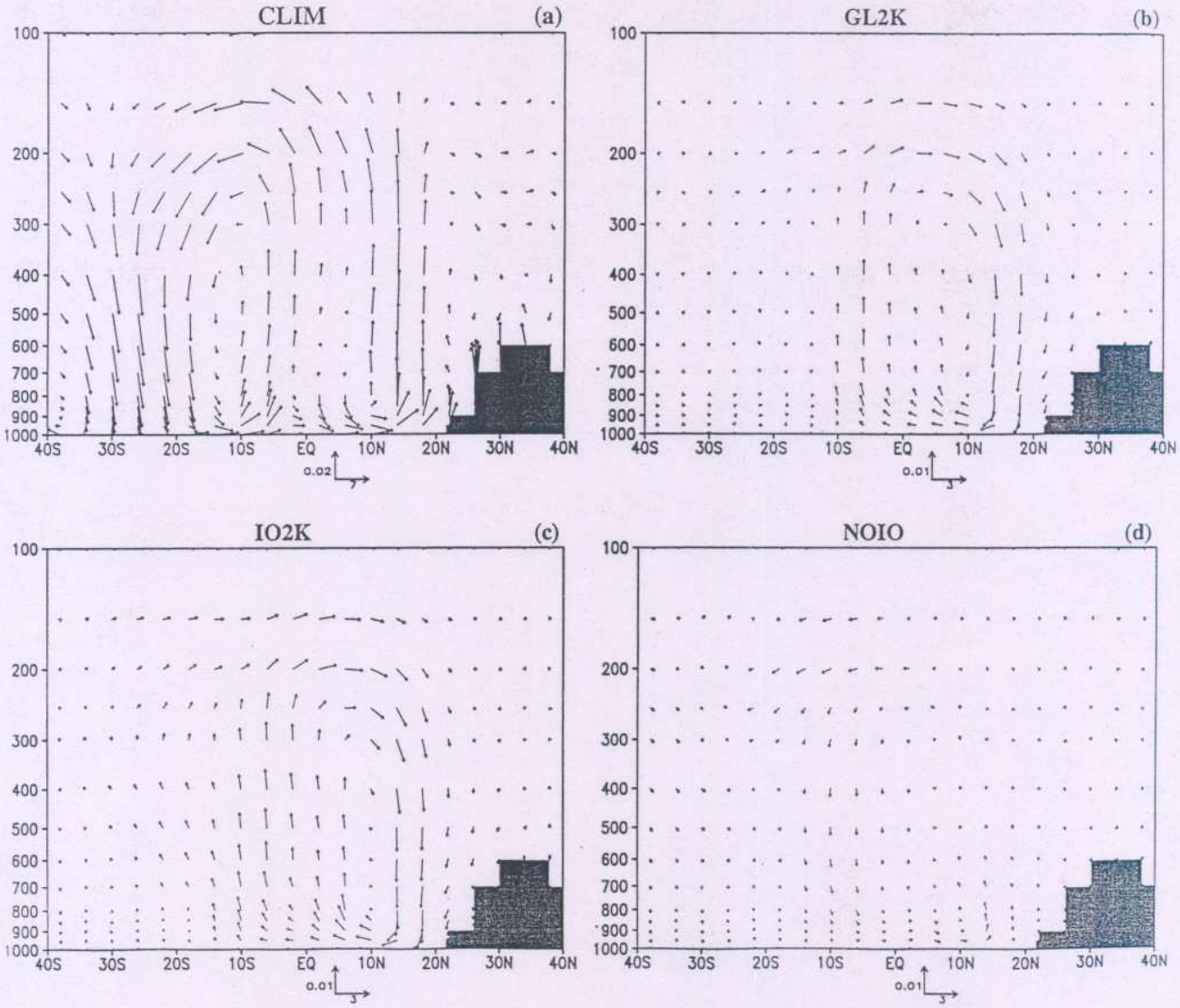

Fig.11. (a) The simulated Monsoon Hadley cell for JJAS months in the CLIM experiment. The meridional wind (ms^{-1}) and vertical wind (hPa s^{-1}) components are averaged longitudinally between 50°-100°E. (b) Same as (a) except for the GL2K anomalies. (c) Same as (a) except for the IO2K anomalies. (d) Same as (a) except for the NOIO anomalies.

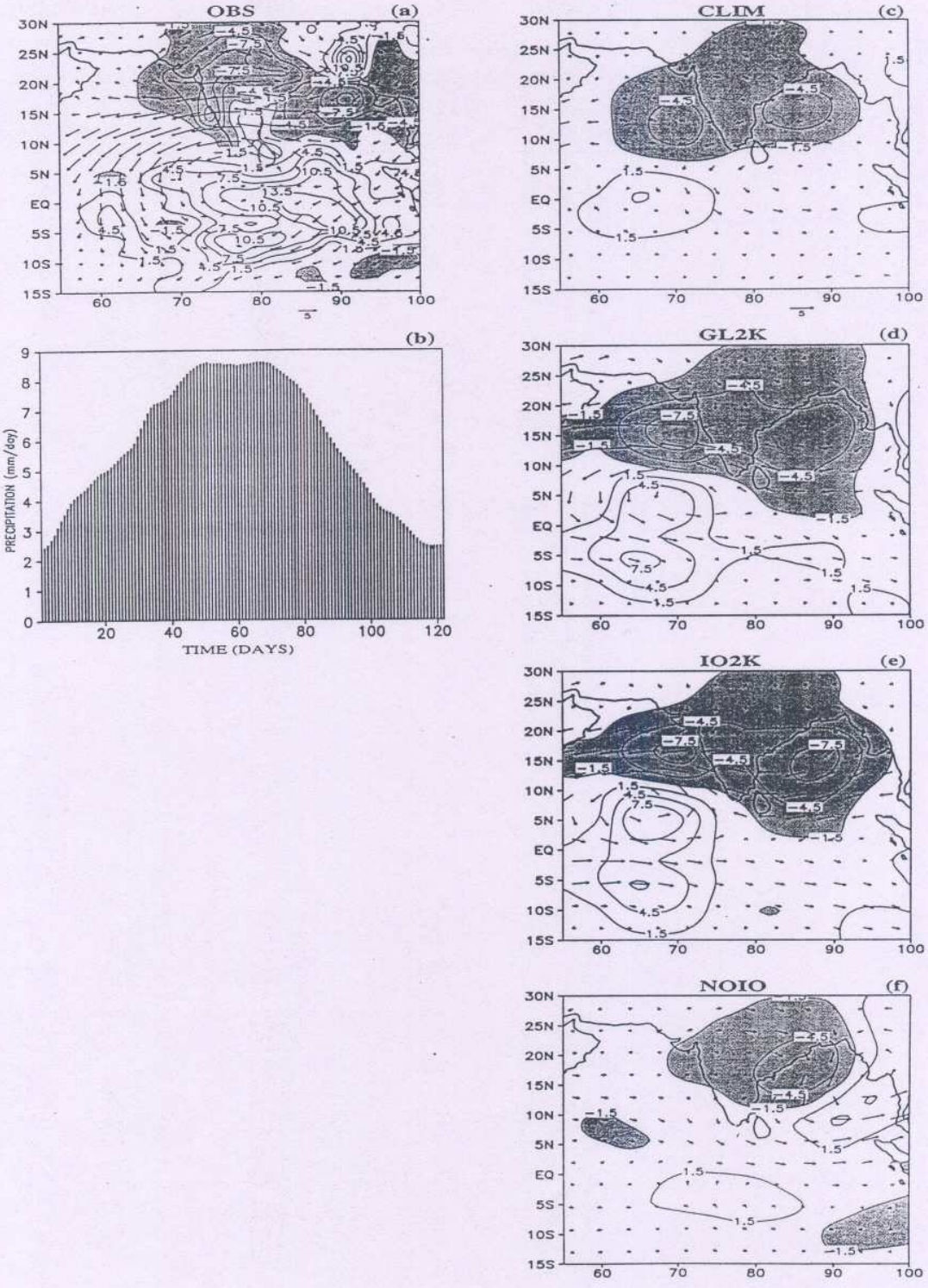

Fig.12. (a) The composited rainfall (mm day^{-1}) anomaly pattern obtained by averaging the CMAP rainfall anomalies over those pentads coinciding with the three major break spells of 2000. (b) Illustration of the time-series of daily rainfall normals averaged over (70-95 °E; 10-30°N) for the COLA GCM from 01 June to 30 September. This time-series is a mean of daily rainfall from 30 cases of CLIM SST runs that were initiated from 30 different atmospheric initial conditions (10 members of 2000; 10 members during May 1987 and 10 members during May 1988). A 3-day running mean is applied on the daily rainfall normals. (c) The composited rainfall anomaly during breaks for the CLIM run. (d) Same as (c) except for GL2K experiment. (e) Same as (c) except for IO2K experiment. (f) Same as (c) except for NOIO experiment.

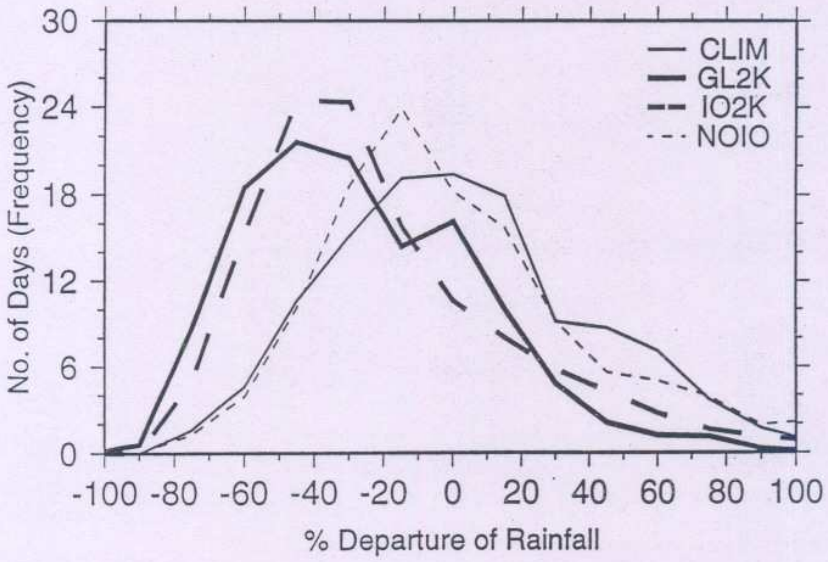

Fig.13 Frequency distribution of daily monsoon rainfall departures in the CLIM, GL2K, IO2K and NOIO simulations. Each curve is an averaged distribution from the 10 ensemble members. The distributions were computed from the daily time-series of rainfall departures over the monsoon region (70-95°E; 10-30°N). Rainfall departures were generated by subtracting the daily climatology (Fig.12b) from the individual realizations.

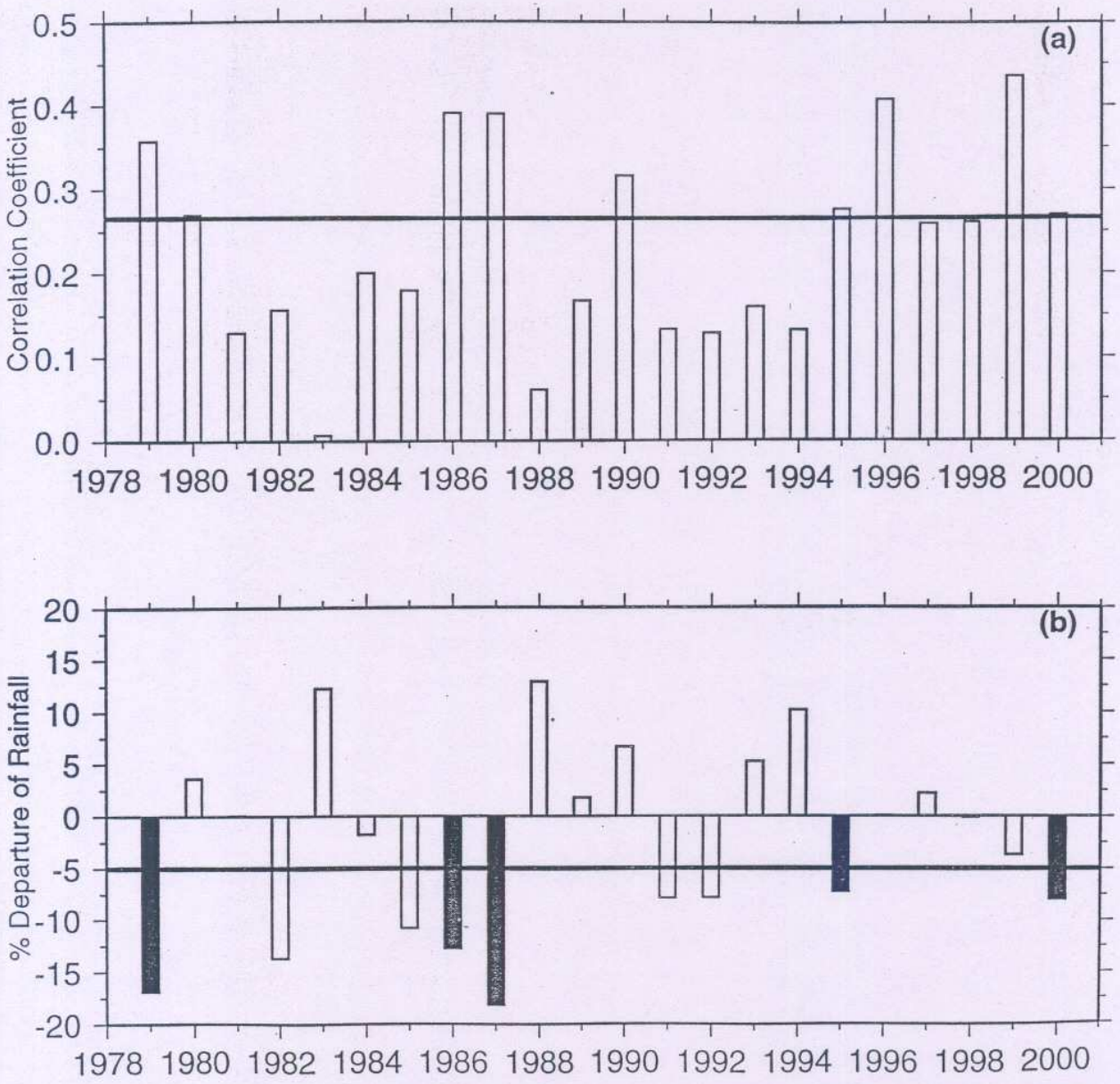

Fig.14. (a) Correlation coefficient (CC) between the observed daily All India Rainfall and daily OLR averaged over (70-100°E; 10°S-EQ) for 22 years (1979-2000). The CCs are computed using the two daily time-series for 93 days (15 Jun - 15 Sep) during each of the 22 monsoon seasons. The 99% significant level of correlation is shown by the solid line (CC=0.266). (b) Histogram of seasonal departures of All India Rainfall (%) from (1979-2000). Solid line represents the 5 % below normal level. Shaded bars are deficient monsoon years selected for making composites.

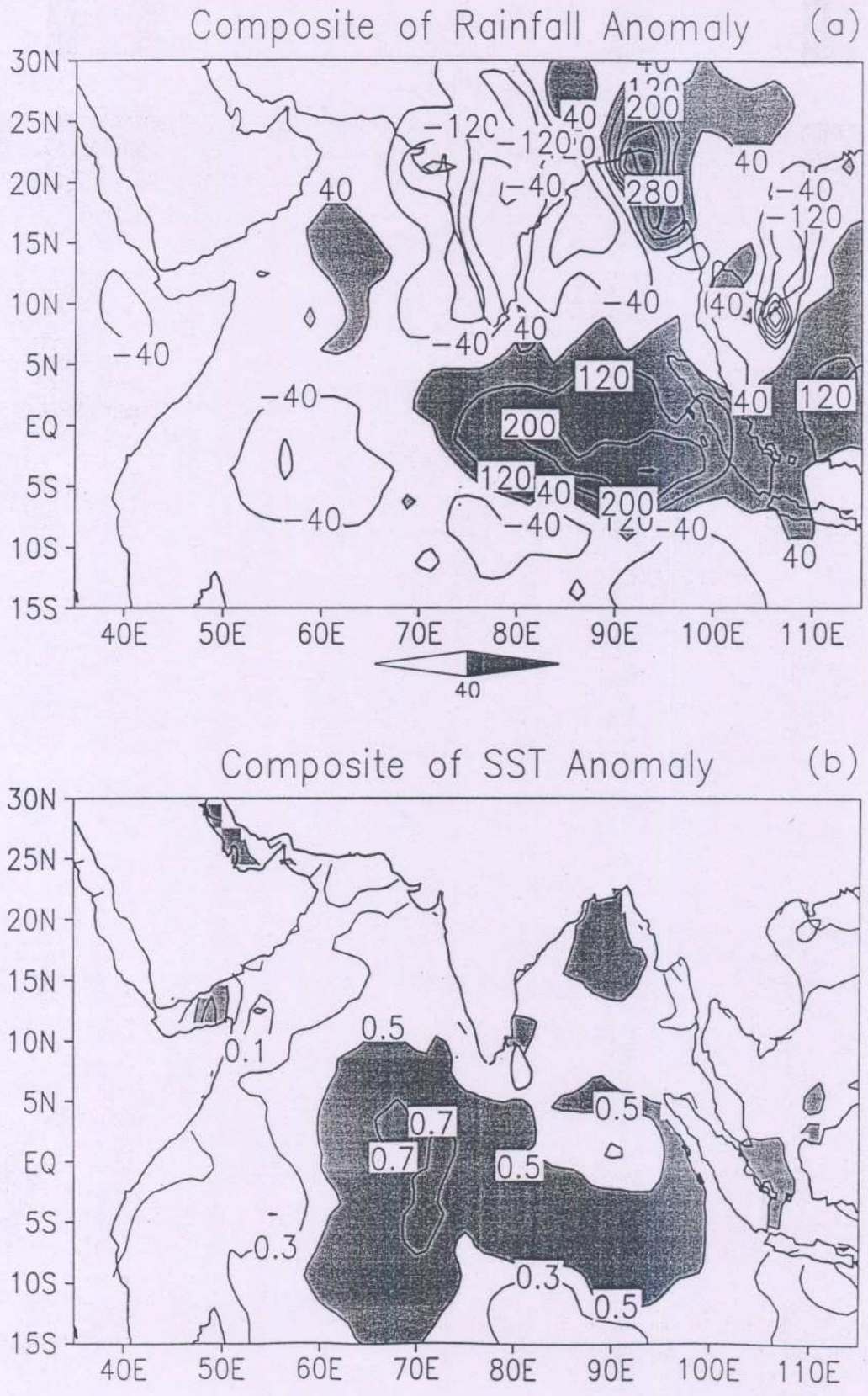

Fig.15. (a) Composite of seasonal (JJAS) rainfall anomaly (mm [illegible]) based on (1979, 1986, 1987, 1995, 2000) from CMAP. (b) Composite of SST anomalies (°C) based on (1986, 1987, 1995, 2000). The OISST is available from November 1981.

I. I. T. M. RESEARCH REPORTS

- Energetic consistency of truncated models, *Asnani G.C.*, August 1971, RR-001.
- Note on the turbulent fluxes of heat and moisture in the boundary layer over the Arabian Sea, *Sinha S.*, August 1971, RR-002.
- Simulation of the spectral characteristics of the lower atmosphere by a simple electrical model and using it for prediction, *Sinha S.*, September 1971, RR-003.
- Study of potential evapo-transpiration over Andhra Pradesh, *Rakhecha P.R.*, September 1971, RR-004.
- Climatic cycles in India-1: Rainfall, *Jagannathan P. and Parthasarathy B.*, November 1971, RR-005.
- Tibetan anticyclone and tropical easterly jet, *Raghavan K.*, September 1972, RR-006.
- Theoretical study of mountain waves in Assam, *De U.S.*, February 1973, RR-007.
- Local fallout of radioactive debris from nuclear explosion in a monsoon atmosphere, *Saha K.R. and Sinha S.*, December 1972, RR-008.
- Mechanism for growth of tropical disturbances, *Asnani G.C. and Keshavamurty R.N.*, April 1973, RR-009.
- Note on "Applicability of quasi-geostrophic barotropic model in the tropics", *Asnani G.C.*, February 1973, RR-010.
- On the behaviour of the 24-hour pressure tendency oscillations on the surface of the earth, Part-I: Frequency analysis, Part-II: Spectrum analysis for tropical stations, *Misra B.M.*, December 1973, RR-011.
- On the behaviour of the 24 hour pressure tendency oscillations on the surface of the earth, Part-III : Spectrum analysis for the extra-tropical stations, *Misra B.M.*, July 1976, RR-011A.
- Dynamical parameters derived from analytical functions representing Indian monsoon flow, *Awade S.T. and Asnani G.C.*, November 1973, RR-012.
- Meridional circulation in summer monsoon of Southeast Asia, *Asnani G.C.*, November 1973, RR-014.
- Energy conversions during weak monsoon, *Keshavamurty R.N. and Awade S.T.*, August 1974, RR-015.
- Vertical motion in the Indian summer monsoon, *Awade S.T. and Keshavamurty R.N.*, August 1974, RR-016.
- Semi-annual pressure oscillation from sea level to 100mb in the northern hemisphere, *Asnani G.C. and Verma R.K.*, August 1974, RR-017.
- Suitable tables for application of gamma probability model to rainfall, *Mooley D.A.*, November 1974, RR-018.

- Annual and semi-annual thickness oscillation in thenorthern hemisphere, *Asnani G.C. and Verma R.K.*, January 1975, RR-020.

- Spherical harmonic analysis of the normal constant pressure charts in the northern hemisphere, *Awade S.T., Asnani G.C. and Keshavamurty R.N.*, May 1978, RR-021.

- Dynamical parameters derived from analytical function representing normal July zonal flow along 87.5 °E, *Awade S.T. and Asnani G.C.*, May 1978, RR-022.

- Study of trends and periodicities in the seasonal and annual rainfall of India, *Parthasarathy B. and Dhar O.N.*, July 1975, RR-023.

- Southern hemisphere influence on Indian rainfall, *Raghavan K.., Paul D.K. and Upasani P.U.*, February 1976, RR-024.

- Climatic fluctuations over Indian region - Rainfall : A review, *Parthasarathy B. and Dhar O.N.*, May 1978, RR-025.

- Annual variation of meridional flux of sensible heat, *Verma R.K. and Asnani G.C.*, December 1978, RR-026.

- Poisson distribution and years of bad monsoon over India, *Mooley D.A and Parthasarathy B.*, April 1980, RR-027.

- On accelerating the FFT of Cooley and Tukey, *Mishra S.K.*, February 1981, RR-028.

- Wind tunnel for simulation studies of the atmospheric boundary layer, *Sivaramakrishnan S.*, February 1981, RR-029.

- Hundred years of Karnataka rainfall, *Parthasarathy B. and Mooley D.A.*, March 1981, RR-030.

- Study of the anomalous thermal and wind patterns during early summer season of 1979 over the Afro-Asian region in relation to the large-scale performance of the monsoon over India, *Verma R.K. and Sikka D.R.*, March 1981, RR-031.

- Some aspects of oceanic ITCZ and its disturbances during the onset and established phase of summer monsoon studied with Monex-79 data, *Sikka D.R., Paul D.K. and Singh S.V.*, March 1981, RR- 032.

- Modification of Palmer drought index, *Bhalme H.N. and Mooley D.A.*, March 1981, RR-033.

- Meteorological rocket payload for Menaka-II/Rohini 200 and its developmental details, *Vernekar K.G. and Brij Mohan*, April 1981, RR-034.

- Harmonic analysis of normal pentad rainfall of Indian stations, *Anathakrishnan R. and Pathan J.M.*, October 1981, RR-035.

- Pentad rainfall charts and space-time variations of rainfall over India and the adjoining areas, *Anathakrishnan R. and Pathan J.M.*, November 1981, RR-036.

- Dynamic effects of orography on the large scale motion of the atmosphere Part I : Zonal flow and elliptic barrier with maximum height of one km., *Bavadekar S.N. and Khaladkar R.M.*, January 1983, RR-037.

- Limited area five level primitive equation model, *Singh S.S.*, February 1983, RR-038.
- Developmental details of vortex and other aircraft thermometers, *Vernekar K.G., Brij Mohan and Srivastava S.*, November 1983, RR-039.
- Note on the preliminary results of integration of a five level P.E. model with westerly wind and low orography, *Bavadekar S.N., Khaladkar R.M., Bandyopadhyay A. and Seetaramayya P.*, November 1983, RR-040.
- Long-term variability of summer monsoon and climatic change, *Verma R.K., Subramaniam K. and Dugam S.S.*, December 1984, RR-041.
- Project report on multidimensional initialization for NWP models, *Sinha S.*, February 1989, RR-042.
- Numerical experiments with inclusion of orography in five level P.E. Model in pressure-coordinates for interhemispheric region, *Bavadekar S.N. and Khaladkar R.M.*, March 1989, RR-043.
- Application of a quasi-lagrangian regional model for monsoon prediction, *Singh S.S. and Bandyopadhyay A.*, July 1990, RR-044.
- High resolution UV-visible spectrometer for atmospheric studies, *Bose S., Trimbake H.N., Londhe A.L. and Jadhav D.B.*, January 1991, RR-045.
- Fortran-77algorithm for cubic spline interpolation for regular and irregular grids, *Tandon M.K.*, November 1991, RR-046.
- Fortran algorithm for 2-dimensional harmonic analysis, *Tandon M.K.*, November 1991, RR- 047.
- 500 hPa ridge and Indian summer monsoon rainfall : A detailed diagnostic study, *Krishna Kumar K., Rupa Kumar K. and Pant G.B.*, November 1991, RR-048.
- Documentation of the regional six level primitive equation model, *Singh S.S. and Vaidya S.S.*, February 1992, RR-049.
- Utilisation of magnetic tapes on ND-560 computer system, *Kripalani R.H. and Athale S.U.*, July 1992, RR-050.
- Spatial patterns of Indian summer monsoon rainfall for the period 1871-1990, *Kripalani R.H., Kulkarni A.A., Panchawagh N.V. and Singh S.V.*, August 1992, RR-051.
- FORTRAN algorithm for divergent and rotational wind fields, *Tandon M.K.*, November 1992, RR-052.
- Construction and analysis of all-India summer monsoon rainfall series for the longest instrumental period: 1813-1991, *Sontakke N.A., Pant G.B. and Singh N.*, October 1992, RR-053.
- Some aspects of solar radiation, *Tandon M.K.*, February 1993, RR-054.
- Design of a stepper motor driver circuit for use in the moving platform, *Dharmaraj T. and Vernekar K.G.*, July 1993, RR-055.

- Experimental set-up to estimate the heat budget near the land surface interface, *Vernekar K.G., Saxena S., Pillai J.S., Murthy B.S., Dharmaraj T. and Brij Mohan,* July 1993, RR-056.

- Identification of self-organized criticality in atmospheric total ozone variability, *Selvam A.M. and Radhamani M.,* July 1993, RR-057.

- Deterministic chaos and numerical weather prediction, *Selvam A.M.,* February 1994, RR-058.

- Evaluation of a limited area model forecasts, *Singh S.S., Vaidya S.S Bandyopadhyay A., Kulkarni A.A, Bawiskar S.M.,Sanjay J., Trivedi D.K. and Iyer U.,* October 1994, RR-059.

- Signatures of a universal spectrum for atmospheric interannual variability in COADS temperature time series, *Selvam A.M., Joshi R.R. and Vijayakumar R.,* October 1994, RR-060.

- Identification of self-organized criticality in the interannual veriability of global surface temperature, *Selvam A.M. and Radhamani M.,* October 1994, RR-061.

- Identification of a universal spectrum for nonlinear veriability of solar-geophysical parameters, *Selvam A.M., Kulkarni M.K., Pethkar J.S. and Vijayakumar R.,* October 1994, RR-062.

- Universal spectrum for fluxes of energetic charged particles from the earth's magnetosphere, *Selvam A.M. and Radhamani M.,* June 1995, RR-063.

- Estimation of nonlinear kinetic energy exchanges into individual triad interactions in the frequency domain by use of the cross-spectral technique, *Chakraborty D.R.,* August 1995, RR-064.

- Monthly and seasonal rainfall series for all-India homogeneous regions and meteorological subdivisions: 1871-1994, *Parthasarathy B., Munot A.A. and Kothawale D.R.,* August 1995, RR-065.

- Thermodynamics of the mixing processes in the atmospheric boundary layer over Pune during summer monsoon season, *Morwal S.B. and Parasnis S.S.,* March 1996, RR-066.

- Instrumental period rainfall series of the Indian region: A documentation, *Singh N. and Sontakke N.A.,* March 1996, RR-067.

- Some numerical experiments on roundoff-error growth in finite precision numerical computation, *Fadnavis S.,* May 1996, RR-068.

- Fractal nature of MONTBLEX time series data, *Selvam A.M. and Sapre V.V.,* May 1996, RR-069.

- Homogeneous regional summer monsoon rainfall over India: Interannual variability and teleconnections, *Parthasarathy B., Rupa Kumar K. and Munot A.A.,* May 1996, RR-070.

- Universal spectrum for sunspot number variability, *Selvam A.M. and Radhamani M.,* November 1996, RR-071.

- Development of simple reduced gravity ocean model for the study of upper north Indian ocean, *Behera S.K. and Salvekar P.S.*, November 1996, RR-072.

- Study of circadian rhythm and meteorological factors influencing acute myocardial infraction, *Selvam A.M., Sen D. and Mody S.M.S.*, April 1997, RR-073.

- Signatures of universal spectrum for atmospheric gravity waves in southern oscillation index time series, *Selvam A.M., Kulkarni M.K., Pethkar J.S. and Vijayakumar R.*, December 1997, RR-074.

- Some example of X-Y plots on Silicon Graphics, *Selvam A.M., Fadnavis S. and Gharge S.P.*, May 1998, RR-075.

- Simulation of monsoon transient disturbances in a GCM, *Ashok K., Soman M.K. and Satyan V.*,August 1998, RR-076.

- Universal spectrum for intraseasonal variability in TOGA temperature time series, *Selvam A.M., Radhamani M., Fadnavis S. and Tinmaker M.I.R.*, August 1998, RR-077.

- One dimensional model of atmospheric boundary layer, *Parasnis S.S., Kulkarni M.K., Arulraj S. and Vernekar K.G.*, February 1999, RR-078.

- Diagnostic model of the surface boundary layer - A new approach, *Sinha S.*, February 1999, RR-079.

- Computation of thermal properties of surface soil from energy balance equation using force - restore method, *Sinha S.*, February 1999, RR-080.

- Fractal nature of TOGA temperature time series, *Selvam A.M. and Sapre V.V.*, February 1999, RR-081.

- Evolution of convective boundary layer over the Deccan Plateau during summer monsoon, *Parasnis S.S.*, February 1999, RR-082.

- Self-organized criticality in daily incidence of acute myocardial infarction, *Selvam A.M., Sen D., and Mody S.M.S.*, Feburary 1999, RR-083.

- Monsoon simulation of 1991 and 1994 by GCM : Sensitivity to SST distribution, *Ashrit R.G., Mandke S.K. and Soman M.K.*, March 1999, RR-084.

- Numerical investigation on wind induced interannual variability of the north Indian Ocean SST, *Behera S.K., Salvekar P.S. and Ganer D.W.*, April 1999, RR-085.

- On step mountain eta model, *Mukhopadhyay P., Vaidya S.S., Sanjay J. and Singh S.S.*, October 1999, RR-086.

- Land surface processes experiment in the Sabarmati river basin: an overview and early results, *Vernekar K.G., Sinha S., Sadani L.K., Sivaramakrishnan S., Parasnis S.S., Brij Mohan, Saxena S., Dharamraj T., Pillai, J.S., Murthy B.S., Debaje, S.B., Patil, M.N. and Singh A.B.*, November 1999, RR-087.

- Reduction of AGCM systematic error by Artificial Neural Network: A new approach for dynamical seasonal prediction of Indian summer monsoon rainfall, *Sahai A.K. and Satyan V.*, December 2000, RR-088.

- Ensemble GCM simulations of the contrasting Indian summer monsoons of the 1987 and 1988, *Mujumdar M. and Krishnan R.*, February 2001, RR-089.

- Aerosol measurements using lidar and radiometers at Pune during INDOEX field phases, Maheskumar R.S., Devara P.C.S., Raj P.E., Jaya Rao Y.,Pandithurai G., Dani K.K., Saha S.K., Sonbawne S.M. and Tiwari Y.K., December 2001, RR-090.